# Title: Mixed Immunotherapy and Chemotherapy of Tumors: Modeling, Applications and Biological Interpretations

L. G. de Pillis (contact author) [a]

[a] *Harvey Mudd College, Claremont, CA 91711, USA.*

*Tel: 909-621-8975. Fax: 909-621-8366.* depillis@hmc.edu

W. Gu [b]

[b] *Harvey Mudd College, Claremont, CA 91711, USA.*

*Tel: 909-621-8929. Fax: 909-621-8366.* gu@math.hmc.edu

A. E. Radunskaya [c]

[c] *Pomona College, Claremont, CA 91711, USA.* aradunskaya@pomona.edu

**Running Title: An Analysis of Mixed Immunotherapy and Chemotherapy**

**Key Words:** Mathematical Modeling, Chemotherapy, Immunotherapy, Vaccine, Cancer, Tumor

**Abstract**

We develop and analyze a mathematical model, in the form of a system of ordinary differential equations (ODEs), governing cancer growth on a cell population level with combination immune, vaccine and chemotherapy treatments. We characterize the ODE system dynamics by locating equilibrium points, determining stability properties, performing a bifurcation analysis, and identifying basins of attraction. These system characteristics are useful not only to gain a broad understanding of the specific system dynamics, but also to help guide the development of combination therapies. Numerical simulations of mixed chemo-immuno and vaccine therapy using both mouse and human parameters are presented. We illustrate situations for which neither chemotherapy nor immunotherapy alone are sufficient to control tumor growth, but in combination the therapies are able to eliminate the entire tumor.

## 1 Introduction and Background

**The Importance of the Immune System and Immunotherapy**. Immunotherapies are quickly becoming an important component in the multi-pronged approaches being developed to treat certain forms of cancer. The goal of immunotherapy is to strengthen the body's own natural ability to combat cancer by enhancing the effectiveness of the immune system. The importance of the immune system in fighting cancer has been verified in the laboratory as well as with clinical experiments. See, for example, [29,70,66,67,85]. Additionally, it is known that those with weakened immune systems, such as those suffering from AIDS, are more likely to contract certain rare forms of cancer. This phenomenon can be interpreted as providing further evidence that the role played by the immune response in battling cancer is critical. See, for example, [16,47].

Through the mathematical modeling of tumor growth, the presence of an immune component has been shown to be essential for producing clinically observed phenomena such as tumor dormancy, oscillations in tumor size, and spontaneous tumor regression. The mathematical modeling of the entire immune system can be an enormously intricate task, as demonstrated in [75], so models that describe the immune system response to a tumor challenge must necessarily focus on those elements of the immune system that are known to be significant in controlling tumor growth. In the work of deBoer and Hogeweg [19], a mathematical model of the cellular immune response was used to investigate such an immune reaction to tumors. It was found that initially small doses of antigens do lead to tumor dormancy. The mathematical model of Kirschner and Panetta [54], which also focuses on the tumor-immune

interaction, indicates that the dynamics among tumor cells, immune cells, and the cytokine interleukin-2 (IL-2) can explain both short-term oscillations in tumor size as well as long-term tumor relapse. The model developed by Kuznetsov [57,56], in which the nonlinear dynamics of immunogenic tumors are examined, also exhibits oscillatory growth patterns in tumors, as well as dormancy and "creeping through": when the tumor stays very small for a relatively long period of time, and subsequently grows to be dangerously large. In these mathematical models, the cyclical behavior of the tumor is directly attributable to the interaction of the tumor with the immune system. There is a host of literature that addresses the development of various mathematical descriptions of cancer and the immune response, among which we mention just a few: [4,5,9,10,25,17,13,55,15,18,24,30–32,34,35,43,52,58,61,64,69,72,82–84,86–89,91,92]. In [22] we also demonstrate the critical role the immune system plays in giving rise to cyclical behavior. This model also highlights the crucial role the immune system plays in the process of tumor elimination.

The clear importance of the immune system in controlling cancer growth, both clinically and mathematically, indicates that models incorporating tumor growth and treatment would do well to include an immune system component. Once this component is in place, it is then possible to model how various immunotherapies may affect the system, either singly or in combination with one another. Recent clinical data have shown there is potential benefit in harnessing the power of the immune system in combination with traditional chemotherapy. For example, in Wheeler et al. [90], it is demonstrated that vaccine therapy in combination with chemotherapy more effectively extends patient survival times than either chemotherapy or vaccine

therapy alone.

**Immunotherapy**.

The clinical evidence for the potential of immune system control of certain malignancies has motivated new research into the development of immunotherapies and vaccine therapies for cancers (see, for example [6],[12],[27],[73],[81],[90]). Immunotherapy falls into three main categories: immune response modifiers, monoclonal antibodies, and vaccines (see, for example, [79]). The first category contains substances that affect immune response, such as interleukins (including IL-2), interferons, tumor necrosis factors (TNF), colony-stimulating factors (CSF), and B-cell growth factors. In the next category, monoclonal antibodies are currently being developed to target specific cancer antigens. These monoclonals can distinguish between normal and cancer cells, and they can then be used to diagnose cancer, as well as to treat tumors by "guiding" anticancer drugs toward the malignant cells (see, e.g., [77,41,60]). In the third category are vaccines, which are generally used therapeutically, and are created from tumor cells. These work by helping the immune system to recognize and attack specific cancer cells. In this work, we implement treatment from the first category in the form of mathematical terms that represent IL-2 and tumor infiltrating lymphocyte (TIL) injections, and additionally incorporate treatment from the third category: new mathematical forms that distinguish between specific and nonspecific immune responses, allowing for the incorporation of a vaccine component into the model. Although monoclonal antibody treatments are considered promising, they are currently not considered in this work.

**Cancer Vaccines**. There are fundamental differences between the use and effects

of antiviral vaccines and anticancer vaccines. While many vaccines for infectious diseases are preventative, cancer vaccines are designed to be used therapeutically, treating the disease after it has begun, and preventing the disease from recurring. Cancer vaccines are still considered to be highly experimental as compared with other forms of cancer immunotherapy, but in early clinical trials are showing increasing promise in their ability to improve the immune response to certain forms of cancer (see, e.g., [79],[90]).

Since cancer vaccines and antiviral vaccines differ in their application, mathematical models of these vaccines should exhibit different dynamics. The goal of this paper is to build on existing models of tumor growth, incorporating an immune system response and expanding these models to include the effect of anti-tumor vaccination and immunotherapies in conjunction with chemotherapies. In another work, the authors will extend this model into a larger framework that incorporates spatial and geometric components.

The outline of this paper is as follows. In section 2 we present the set of assumptions incorporated into our tumor growth model, and develop the system of ODEs that form the mathematical model. In section 3, we discuss how parameter values for the model are chosen. In section 4, we carry out an analysis of the non-dimensionalized model, finding equilibrium points, stability criteria, bifurcation points, and basins of attraction. Section 5 presents numerical experiments based on parameters representing data collected from laboratory mice, and includes contrasts between immunotherapies and chemotherapies. In section 6 we present numerical experiments that reflect parameter values gathered from human clinical trials, again contrasting

immunotherapies with chemotherapies, and simulating combinations of these. In section 7 we present theoretical simulations highlighting the potential effect of vaccine therapy on a patient, as well as vaccine therapy in combination with chemotherapy. In section 8 we summarize and discuss our conclusions.

## 2 Model Formulation

One goal for a mathematical model is to allow for sufficient complexity so that the model will qualitatively generate clinically observed *in vivo* tumor growth patterns, while it simultaneously maintains sufficient simplicity to admit analysis. The model we present in this paper can exhibit the following behaviors in the absence of medical interventions:

(1) Tumor dormancy and sneaking through. There is clinical evidence that a tumor mass may disappear, or at least become no longer detectable, and then for reasons not yet fully understood, may reappear, growing to lethal size.
(2) Uncontrolled growth of tumor cells due to accelerated growth rates.
(3) Detrimental effects of immune cells on tumor cells through normal immune function.
(4) Inactivation of cytotoxic immune cells through interaction with tumor cells.
(5) Global stimulatory effect of tumor cells on the immune response.
(6) Both nonspecific and specific immune responses to the presence of tumor cells.

Additionally, since we wish to determine improved combination therapy treatment protocols, we include the following mathematical model components that represent

tumor response to medical interventions.

(1) System response to chemotherapy (direct cytotoxic effects on tumor and immune cell populations).
(2) System response to direct immunotherapy (such as IL-2 and tumor infiltrating lymphocyte (TIL) injections).
(3) System response to vaccine therapy (including direct stimulatory effects on the immune system through injection of modified autologous tumor cells).

The model is a system of ordinary differential equations whose state variables are populations of tumor cells, specific and nonspecific immune cells, and concentrations of therapeutic interventions. The assumptions that were used to determine the model equations are outlined below, followed by a discussion of the model equations themselves.

### *2.1 Model Assumptions*

The ODE model is based on that originally developed by de Pillis and Radunskaya [23], and is now extended by adding new cell interaction terms as well as terms describing chemotherapy and immunotherapy. For the sake of completeness, we outline the assumptions of the original model here. We should note that there is not universal agreement as to the underlying dynamics or precise cascades of events that take place in the immune response process. Our assumptions, therefore, are based on published statements and conjectures as well as reasonable suppositions.

- A tumor grows logistically in the absence of an immune response. This is one accepted growth model for tumors [7], and is also based on fittings of the data in [26].

- Both NK and $CD8^+$T cells are capable of killing tumor cells. (See, for example, [26],[51], [37].)

- Both NK and $CD8^+$T cells respond to tumor cells by expanding and increasing cytolytic activity. (See, for example, [71,53])

- NK cells are normally present in the body, even when no tumor cells are present, since they are part of the innate immune response. See, for example, [78].

- As part of the specific immune response, active tumor-specific $CD8^+$T cells are only present in large numbers when tumor cells are present. (See, for example, [78], [54])

- NK and $CD8^+$T cells become inactive after some number of encounters with tumor cells. (See, for example, [1].)

The following additional assumptions are used in the development of therapeutic terms.

- Circulating lymphocyte levels can be used as a measure of patient health (see, e.g.,[68,65,40]). Components of the lymphocyte population are involved in the production of antibody and in stimulating B-cells. NK cells kill cells to which antibody has attached (in addition to killing cells lacking MHC-I surface

molecules). In this model, the source of the NK cell population is represented as a fraction of the circulating lymphocyte population, a simplification meant to represent the complex cascade of biological events that leads to NK cell stimulation (see, eg, [11]).

- The fraction of the tumor population killed by chemotherapy depends on the amount of drug in the system. The fraction killed has a maximum less than one, since only tumor cells in certain stages of development can be killed by chemotherapy [74].

- A fraction of NK cells, $CD8^{+}$T cells, and circulating lymphocytes are also killed by chemotherapy, according to a similar fractional kill curve [33].

- NK and T cells are components of the process of stimulation and elimination of activated effector cells, a model simplification meant to reflect the self-regulatory nature of the immune system (see, e.g.,[28],[37],[50]).

### *2.2 ODE Model: General Form of Equations*

The model describes the kinetics of four populations (tumor cells and three types of immune cells), as well as two drug concentrations in the bloodstream, using a series of coupled ordinary differential equations based on the model developed by de Pillis and Radunskaya [23]. The populations at time $t$ are denoted by:

- $T(t)$, tumor cell population

- $N(t)$, total NK cell population

- $L(t)$, total CD8$^+$T cell population
- $C(t)$, number of circulating lymphocytes (or white blood cells)
- $M(t)$, chemotherapy drug concentration in the bloodstream
- $I(t)$, immunotherapy drug concentration in the bloodstream

The equations governing the population kinetics must take into account a net growth term for each population ($G_T$, $G_N$, $G_L$, $G_C$, $G_M$, $G_I$), the fractional cell kill ($F_N$, $F_L$, $F_{MT}$, $F_{MN}$, $F_{ML}$, $F_{LI}$, $F_{CM}$), per cell recruitment ($R_N$, $R_L$), cell inactivation ($I_N$, $I_L$) and external intervention with medication ($H_L$, $H_M$, $H_I$). We attempt to use the simplest expressions for each term that still accurately reflect experimental data and recognize population interactions.

Note that the population levels of NK and CD8$^+$T cells actually represent immune cell "effectiveness" in the sense that an increase in the total population count in the mathematical model may actually be evidenced biologically either as a greater number of total cells, or as each individual immune cell becoming more efficient at killing the target tumor cells.

The functional forms that we choose for each cell-interaction term are discussed below. We have chosen to represent parameters by lower case letters always assumed to be positive, and state variables or functions of state variables by upper case letters.

**Growth and Death Terms** We adapt the growth terms for tumor and CD8$^+$T cells from [23]. Tumor growth is assumed to be logistic, based on data gathered from

immunodeficient mice [26]. Therefore $G_T = aT(1 - bT)$. Cell growth for CD8$^+$T cells consists only of natural death rates, since no CD8$^+$T cells are assumed to be present in the absence of tumor cells, so $G_L = -mL$.

The model in [23] assumed a constant NK cell production rate. In the new model, this growth term is tied to the overall immune health levels as measured by the population of circulating lymphocytes. This allows for the suppression of stem cells during chemotherapy, which lowers circulating lymphocyte counts and affects the production rate of NK cells. Therefore, $G_N = eC - fN$. We assume that circulating lymphocytes are generated at a constant rate, and that each cell has a natural lifespan. This gives us the term $G_C = \alpha - \beta C$. We assume that the chemotherapy drug, after injection, will be eliminated from the body over time at a rate proportional to its concentration, giving an exponential decay: $G_M = -\gamma M$. Similarly, we assume the immunotherapy drug, interleukin-2 (IL-2), decays exponentially: $G_I = -\mu_I I$.

**Fractional Cell Kill Terms**

The fractional cell kill terms for $N$ and $L$ are taken from de Pillis et al.[23]. These fractional cell kill terms represent negative interactions between two populations. They can represent competition for space and nutrients as well as regulatory action and direct cell population interaction. The interaction between tumor and NK cells takes the form $F_N(T, N) = -cNT$. Tumor lysis by CD8$^+$T cells, on the other hand, has the form:

$$F_L(T, L) = d\frac{(L/T)^l}{s + (L/T)^l}T.$$

Letting $D(T, L) = d\dfrac{(L/T)^l}{s + (L/T)^l}$, we have $F_L(T, L) = DT$.

The model includes a chemotherapy drug kill term in each of the cell population equations. Certain chemotherapeutic drugs, such as doxorubicin, are only effective during certain phases of the cell cycle, and pharmacokinetics also indicate that the effectiveness of chemotherapy is bounded. We therefore use a saturation term $1-e^{-M}$ to represent the chemotherapy fractional cell kill. Note that at relatively low concentrations of drug, the kill rate is nearly linear, while at higher drug concentration, the kill rate plateaus. The mathematical term we use reflects the dose-response curves suggested by the literature [33]. We therefore let $F_{M\phi} = K_\phi(1 - e^- M)\phi$, for $\phi = T, N, L, C$.

Additionally, we include $CD8^+$T activation by interleukin-2 (IL-2) immunotherapy. This "drug" is actually a naturally occurring cytokine in the human body, and its effect on the immune system's efficacy is described mathematically with a Michaelis-Menten interaction term in the equation for $L$. The presence of IL-2 stimulates the production of $CD8^+$T cells, so we let $F_{LI} = \dfrac{p_I L I}{g_I + I}$. This is the activation term developed in Kirschner's tumor-immune model [54].

**Recruitment**

The recruitment of NK cells takes on the same form as the fractional cell kill term, $D$, for $CD8^+$T cells, with $l$ equal to two, as described by de Pillis and Radunskaya [23]. Hence the NK cell recruitment term is

$$R_N(T, N) = g\frac{T^2}{h + T^2}N.$$

This is a modified Michaelis-Menten term, commonly used in tumor models to govern cell-cell interactions [57], [23], [54].

$CD8^+$T cells are thought to be activated by a number of triggers, including fragments of tumor cells that have been lysed by other $CD8^+$T cells [46]. The $CD8^+$T cell recruitment term has a form similar to that for the NK cell recruitment, except that the tumor population is replaced with the lysed tumor population from the tumor-$CD8^+$T cell interaction term, $D(T, L)$. Thus the new recruitment term is:

$$R_L(T, L) = j\frac{D^2T^2}{k + D^2T^2}.$$

$CD8^+$T cells may also be recruited by the debris from tumor cells lysed by NK cells (see, e.g., [46]). This recruitment term is proportional to the number of cells killed: $R_L(N, T) = r_1NT$. The immune system is also stimulated by the presence of tumor cells to produce more $CD8^+$T cells. Recognition of the presence of the tumor is proportional to the average number of encounters between circulating lymphocytes and the tumor: $R_L(C, T) = r_2CT$.

**Inactivation Terms**

Inactivation of cytolytic potential occurs when an NK or $CD8^+$T cell has interacted with tumor cells several times and ceases to be effective. We use the inactivation terms developed by de Pillis and Radunskaya [23]: $I_N = -pNT$ and $I_L = -qLT$. The parameters in the inactivation terms represent mean inactivation rates.

The third inactivation term, $I_{CL} = -uNL^2$, describes regulation and suppression of $CD8^+$T cell activity, which occurs when there are very high levels of activated

$CD8^+$T cells without responsiveness to cytokines present in the system (see, e.g., [39], [38]). This term comes into play when the amount of $CD8^+$T cells in the body is high, and experimental data document that these cells can become rapidly inactivated even with a tumor present [80]. The cytokine IL-2 aids in the resistance of the $CD8^+$T cell population to this inactivation [2].

**Drug Intervention Terms**

The tumor infiltration lymphocyte (TIL) drug intervention term, $H_L$, for the $CD8^+$T cell population represents an immunotherapy in which the immune cell levels are boosted by the addition of antigen-specific cytolytic immune cells. $H_L$ is a function of time denoted by $v_L = v_L(t)$. Similarly, the drug intervention terms in the equations for $dM/dt$ and $dI/dt$ reflect the amount of chemotherapy and immunotherapy drug given over time. Therefore, drug intervention terms $H_M$ and $H_I$ are also functions of time denoted, respectively, by $v_M = v_M(t)$ and $v_I = v_I(t)$.

### *2.3 ODE Model: Specific Terms in Equations*

Bringing together the specific forms for each cell growth and interaction term leads to the full system of equations:

$$\frac{dT}{dt} = aT(1-bT) - cNT - DT - K_T(1-e^{-M})T \tag{1}$$

$$\frac{dN}{dt} = eC - fN + g\frac{T^2}{h+T^2}N - pNT - K_N(1-e^{-M})N \tag{2}$$

$$\frac{dL}{dt} = -mL + j\frac{D^2T^2}{k+D^2T^2}L - qLT + (r_1N + r_2C)T \tag{3}$$

$$- uNL^2 - K_L(1-e^{-M})L + \frac{p_I LI}{g_I + I} + v_L(t) \tag{4}$$

$$\frac{dC}{dt} = \alpha - \beta C - K_C(1-e^{-M})C \tag{5}$$

$$\frac{dM}{dt} = -\gamma M + v_M(t) \tag{6}$$

$$\frac{dI}{dt} = -\mu_I I + v_I(t) \tag{7}$$

$$D = d\frac{(L/T)^l}{s + (L/T)^l} \tag{8}$$

## 3 Experimental Data and Parameter Derivation

While a general model with non-specific parameters is useful in studying the qualitative dynamics of cancer growth, it is also necessary to study parameter sets meant to reflect specific cancer types (such as melanoma). System parameters can vary greatly from one individual to another, so multiple data sets can be used in order to obtain acceptable parameter ranges. In this work, we use the data made available from both the murine experimental studies of [26] and the human clinical trials of [28]. When necessary, we also use previous model parameters that have been fitted

to experimental curves [21,20,23,57]. Simulations with several sets of parameters were performed in order to evaluate the qualitative behavior of the model [1]. Parameters which were estimated specifically for this investigation are described in the sections below.

### *3.1 Chemotherapy Parameters*

Chemotherapy strength was assumed to be one log-kill, as described in [76], and the values of the kill parameters $K_T, K_N, K_L$ were chosen accordingly. Certain chemotherapy drugs, such as doxorubicin, kill cells by disrupting the process of division and growth. Rapidly dividing cells, like those of the hair, the stomach lining, and the bone marrow where immune cells are produced, are preferentially damaged by chemotherapy (see, e.g., [49], [45]). High doses of drug can also damage other tissues in the body [45]. Ideally, chemotherapy should more effectively kill tumor cells than immune cells. Therefore, $K_N, K_L$, and $K_C$ are assumed to be smaller than $K_T$, but of the same order of magnitude.

The drug decay rate, $\gamma$, was calculated from the drug half-life and the relation $\gamma = \frac{\ln 2}{t_{1/2}}$. The drug half-life, $t_{1/2}$, was estimated to be about 18 hours, based on experimental data for the chemotherapeutic drug doxorubicin [8].

[1] See Tables 1 and 2 for a full listing all of the parameters with their units and descriptions.

### *3.2 Additional CD8$^+$ T cell regulation parameters*

In addition to chemotherapy, we introduce immunotherapy into the system of differential equations. The cytokine interleukin 2 (IL-2) is known to stimulate CD8$^+$T cell recruitment and proliferation (see, e.g., [78]). IL-2 is produced naturally by the body, and is also administered therapeutically to boost immune system function. IL-2 has been used in clinical trials on its own, in combination with chemotherapy, and in conjunction with TIL (tumor infiltrating lymphocyte) injections, in which a large number of highly activated CD8$^+$T cells are injected into the system [80], [14], [42] [62].

The three parameters, $p_I$, $g_I$, $\mu_I$, mirror those of Kirschner's model [54] with minor alterations to reflect the fact that we are only concerned with the amount of IL-2 that is not naturally produced by the immune system. The half-life, $\ln 2/\mu_I$ is taken from Kirschner's model.

The values of $r_2$ and $u$ are chosen to allow for reasonable simulation outcomes of the model.

## 4 Non-Dimensionalization and Analysis

To allow for analysis, we now consider the system of equations (1)-(8) in the absence of treatment. When chemotherapy and immunotherapy are eliminated, the model is reduced to a four-population system of ordinary differential equations. To further clarify the dependence of the system on parameters, and to improve the performance

of numerical methods, we non-dimensionalize the system as follows. Let the non-dimensionalized state variables be

$$C^* = \frac{a}{\alpha}C, \quad T^* = bT, \quad N^* = \frac{a^2}{\alpha e}N, \quad L^* = bL, \quad D^* = \frac{1}{a}D, \quad t^* = at$$

and the corresponding parameters be

$$c^* = \frac{c\alpha e}{a^3}, d^* = \frac{d}{a}, f^* = \frac{f}{a}, g^* = \frac{g}{a}, h^* = hb^2, j^* = \frac{j}{a}, k^* = (kb^2)/a, m^* = \frac{m}{a},$$

$$p^* = \frac{p}{ab}, q^* = \frac{q}{ba}, r_1^* = \frac{r_1\alpha e}{a^3}, r_2^* = \frac{r_2\alpha}{a^2}, s^* = s, u^* = \frac{u\alpha e}{a^3 b}, \beta^* = \frac{\beta}{a}.$$

Leaving the other parameters unchanged, and dropping the stars for notational clarity, the non-dimensionalized system is given by

$$\frac{dT}{dt} = T(1-T) - cNT - DT \tag{9}$$
$$\frac{dN}{dt} = C - fN + g\frac{T^2}{h+T^2}N - pNT \tag{10}$$
$$\frac{dL}{dt} = -mL + j\frac{D^2T^2}{k+D^2T^2}L + (r_1N + r_2C)T - qLT - uNL^2 \tag{11}$$
$$\frac{dC}{dt} = 1 - \beta C \tag{12}$$
$$D = \frac{d(L/T)^l}{s + (L/T)^l} \tag{13}$$

### *4.1 Determination of Equilibria and their Stability*

In order to study the equilibria of the system and their stability, we note first that equation (12) decouples from (9)-(11), so that at equilibrium, we have $C_E = 1/\beta$. This leaves a system of three equations, (9)-(11), which we set simultaneously equal

to zero in order to find the equilibria.

Equation (9) has one zero at the "tumor-free" equilibrium at $T_E = 0$, and possibly several non-zero tumor equilibria. The tumor-free equilibrium for all four state variables is given by $(T_E, N_E, L_E, C_E) = (0, \frac{1}{\beta f}, 0, \frac{1}{\beta})$. Let $E_0$ represent the point $(0, \frac{1}{\beta f}, 0, \frac{1}{\beta})$.

In the case where $T_E \neq 0$, the equilibria are still determined by finding the simultaneous solutions of equations (9), (10) and (11), but in this case, values of equilibrium points for a non-zero tumor must be found numerically.

In particular, setting equation (10) to zero and solving for $N$ yields

$$N_E = \frac{C_E(h + T^2)}{fh + (f - g)T^2 + phT + pT^3} \tag{14}$$

Similarly, requiring that equation (9) equal zero gives

$$D_E = 1 - T - N_E \tag{15}$$

Using this expression in equation (13) gives an expression for $L$:

$$L_{E1} = \left(\frac{D_E s T^l}{d - D_E}\right)^{1/l}, \tag{16}$$

Finally, setting equation (11) to zero gives

$$L^2(uN_E) + \left(m - \frac{jD_E^2T^2}{k + D_E^2T^2} + qT\right)L - (r_1N_E + r_2C_E)T = 0, \tag{17}$$

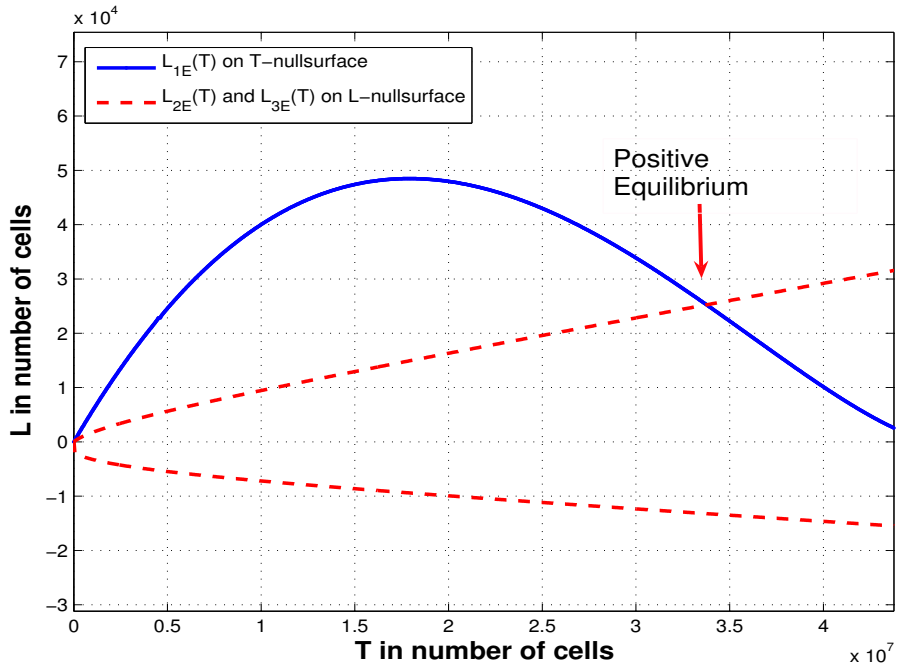


Fig. 1. The non-zero equilibria are the intersections of the graphs of the functions $L(T)$ obtained by finding the equations of the null-surfaces. There is only one non-zero positive equilibrium for the estimated parameter set.

which is quadratic in $L$. Equilibrium points of system (9)-(13) are found by intersecting (16) and (17).

Observe from equations (14) through (17) that there can be multiple non-zero tumor equilibrium points. For the estimated set of mouse parameters, although there are two solutions, there is only one positive (biologically relevant) solution to equations (14) through (17). These solutions are graphed in Figure 1. As a system parameter is changed, other non-zero equilibria can appear (see Figure 2), or negative equilibria can become positive, and therefore biologically feasible.

Stability of the equilibria are determined by linearizing the system about the calculated values, and by determining the stability of the linearized system. The stability of equilibria is important from a physiological viewpoint. If the system is in equilib-

rium, but the equilibrium point is *unstable*, a small perturbation from equilibrium will cause the system to move away from that point and evolve toward the stable equilibrium. This effect is illustrated in Figure 3. At the estimated parameter values, the tumor-free equilibrium is unstable, while the high-tumor equilibrium is stable. The stability of the high-tumor equilibrium implies that, if treatment is stopped, the system will inevitably return to the high-tumor state, *i.e.* the tumor will escape immune surveillance *unless every single tumor cell is killed*. Thus, in a case such as ours for which there are only two equilibria, if the tumor-free equilibrium is unstable, then in order to realistically effect a cure, any treatment must not only reduce the tumor burden, but it must also change the parameters of the system itself. The role of immunotherapy, therefore, might be interpreted in this context as a treatment which changes system parameters by, for example, permanently raising the cytolytic potential of the natural killer cells. We note that if the system were one that admitted a very small but stable tumor, then another "healthy" state might be one for which it is possible to maintain the system at this low tumor level.

### *4.2 Bifurcation analysis*

At the tumor-free equilibrium, $E_0 = (0, \frac{1}{\beta f}, 0, \frac{1}{\beta})$, the Jacobian matrix becomes:

$$\begin{bmatrix} 1 - \frac{c}{\beta f} & 0 & 0 \\ -\frac{p}{\beta f} & -f & 0 \\ \frac{r_1}{\beta f} + \frac{r_2}{\beta} & 0 & -m \end{bmatrix}$$

The eigenvalues of the system linearized about the tumor-free equilibrium are therefore:

$$\lambda_1 = 1 - \frac{c}{\beta f}, \quad \lambda_2 = -f, \quad \lambda_3 = -m$$

Since $f, m > 0$, $\lambda_2$ and $\lambda_3$ are always negative, the tumor-free equilibrium $E_0$ is stable if and only if $\lambda_1 = 1 - \frac{c}{\beta f} < 0 \Leftrightarrow c > \beta f$.

The bifurcation diagram in Figure 2 shows the disappearance of a two unstable non-zero tumor equilibria and the stabilization of the tumor-free equilibrium as the parameter $c$ is increased. Recall that the parameter $c$ represents the effectiveness of the NK cells in lysing the tumor cells. Figure 2 shows a bifurcation point near $c = 1.4 \times 10^{-6}$, after which the progression of the disease is very sensitive to the initial tumor size. This sensitivity is shown in Figure 3, Top, which displays two different scenarios for initial tumor sizes that differ by 1 cell. In one case, the tumor grows to the high equilibrium, and in the other case the tumor population goes to the zero equilibrium. In Figure 3, Bottom, shows two simulations. The dotted line illustrates the case in which $c$ is smaller than the bifurcation value, so that the zero equilibrium is unstable. In this case, one tumor cell can grow to a large tumor mass greater than $2 \times 10^{15}$ cells in sixty days. However, as illustrated by the solid line, if $c$ is larger than the bifurcation value, the zero tumor equilibrium becomes stable and a single tumor cell will die.

Similar analyses can be performed using any of the system parameters in order to determine conditions for the appearance or disappearance of equilibria and to determine equilibrium stability. For example, Figure 4 shows a bifurcation diagram for the $CD8^+$ recruitment parameter, $j$. In this case, the mouse parameters are

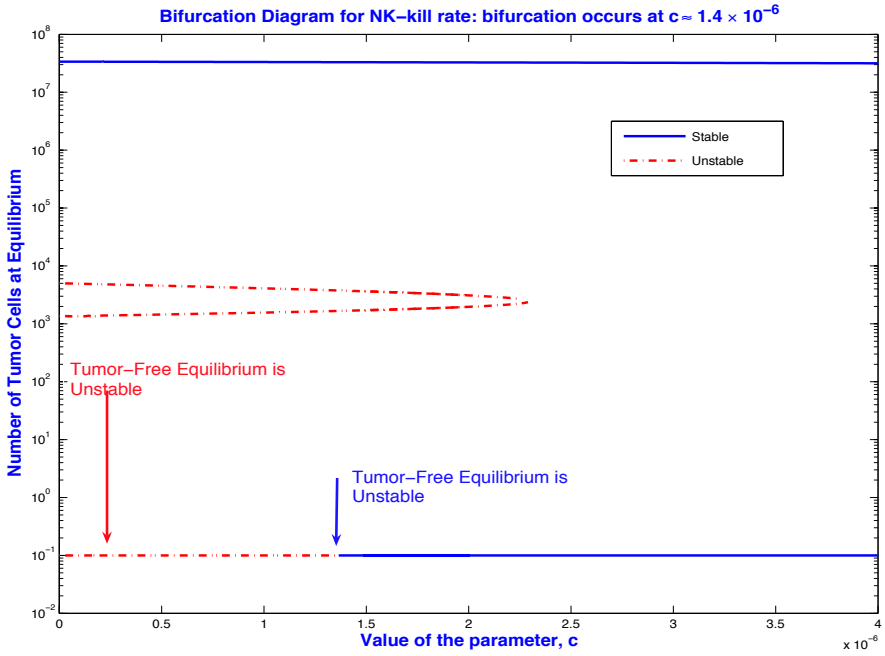


Fig. 2. Bifurcation diagram showing the effect of varying the NK-kill rate, $c$. Other parameters for this diagram are from Table 1.

again used, except that all the tumor-specific immune-cell recruitment terms are initially set to zero (that is, $g = r_1 = r_2 = 0$), in order to isolate the effect of the antigen-specific $CD8^+$ response influenced by $j$. The parameter $j$ is then gradually increased from 0 to 7.

Two bifurcations are evident in the diagram: the first is a *transcritical* bifurcation, where the negative equilibrium becomes positive, and the zero-tumor equilibrium changes its stability. Before the bifurcation, the zero-tumor equilibrium is strictly unstable: even one tumor cell will result in the system moving toward the high-tumor equilibrium. After the bifurcation, the immune system is able to control small initial tumor populations, as long as there is some antigen-specific immune response. Only when the tumor-specific $CD8^+$ population is zero does a very small initial tumor population escape immune surveillance. Initial tumor populations which are

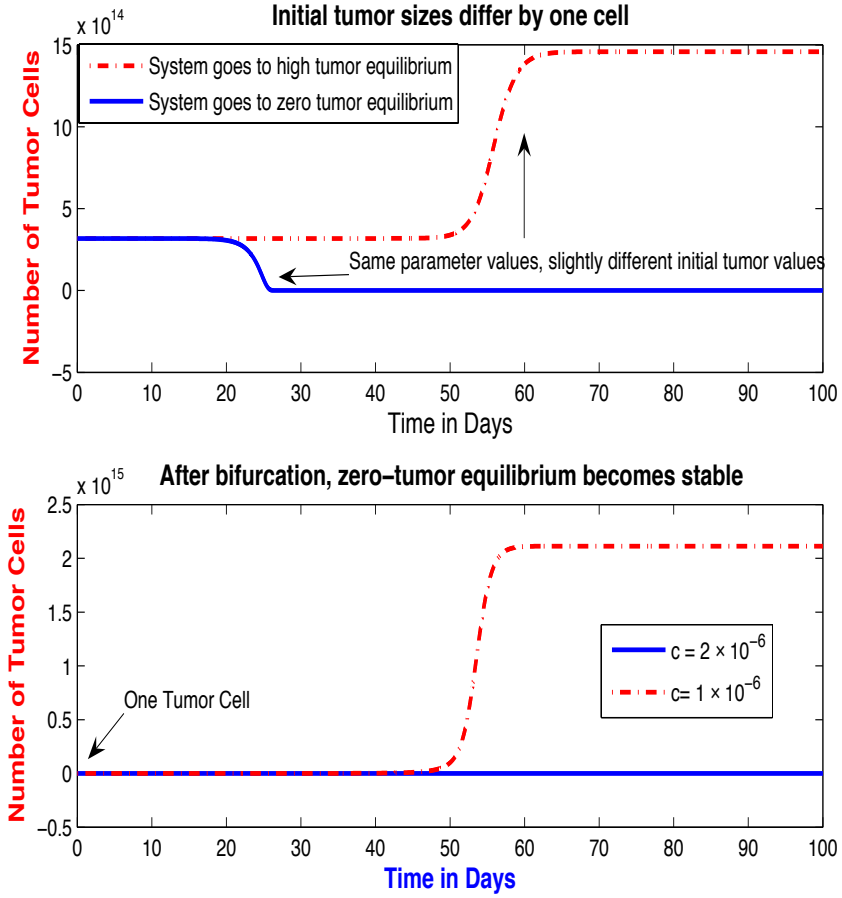


Fig. 3. Simulations illustrating system behavior for three values of parameter $c$. The bifurcation point is $c \approx 1.4x10^{-6}$. **Top:** After the bifurcation point, at $c = 4x10^{-6}$, the system shows sensitivity to initial conditions. In this simulation, a one cell difference in the initial number of tumor cells, $T_0$, results in very different outcomes. Initial values for the state variables are $T_0 \approx 6.89x10^6$, $N_0 \approx 3.97x10^9$, $L_0 \approx 7.15x10^3$, $C_0 \approx 1.65x10^9$. All parameters besides $c$ are from Table 1. **Bottom:** Before the bifurcation, at $c = 1x10^{-6}$, one tumor cell grows to the high tumor equilibrium of approximately $2.1x10^15$ in 60 days. After the bifurcation, at $c = 2x10^{-6}$, an initial value of one tumor cell is drawn to the now stable zero tumor equilibrium. Immune recruitment parameters, $g$, $j$, $r_1$ and $r_2$ are set to zero. With the exception of the values for $c$ and the immune recruitment parameters, all other parameters are from Table 1. Initial values for the state variables are $T_0 = 1$, $N_0 = 1.73x10^{10}$, $L_0 = 0$, $C_0 \approx 1.65x10^9$.

controlled are said to be in the *basin of attraction* of the zero-tumor equilibrium. On the other hand, those which escape immune surveillance, leading the system toward the high-tumor equilibrium, are said to be in the basin of attraction of the high-tumor equilibrium. These basins are shown in Figure 5. Note that since the state-space of the system is actually four-dimensional, what is depicted in Figure 5

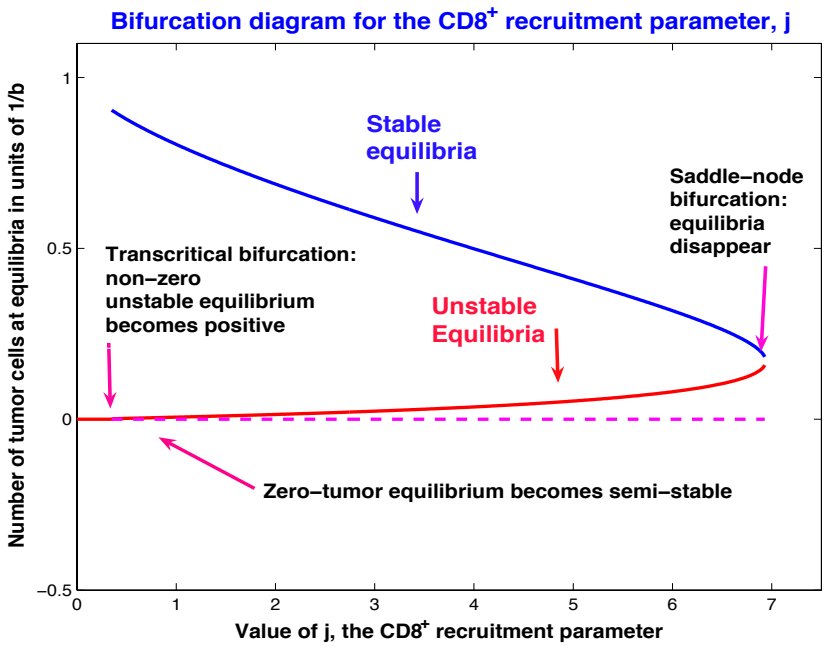


Fig. 4. As the parameter representing the strength of the antigen-specific immune response is varied, system equilibria appear and change their stability

is the projection of the basins onto the Tumor-CD8$^+$-plane, where the values of $N$ and $C$ are kept at their zero-equilibrium values. Figure 5 highlights the fact that even if the tumor is very small, extremely low CD8$^+$T levels will allow the tumor to escape immune surveillance. The location of the basin boundary is therefore crucial in determining the outcome of the disease. In the case of a patient who has undergone chemotherapy which reduces both tumor and CD8$^+$T cell levels, if these levels place the system below the basin boundary then even an undetectable tumor will regrow. However, if the patient is given immunotherapy subsequent to chemotherapy, thereby boosting CD8$^+$T levels above the basin boundary, the system will evolve toward the stable zero-tumor equilibrium, and the tumor will not regrow. This hypothetical scenario emphasizes the potential importance of combination therapy.

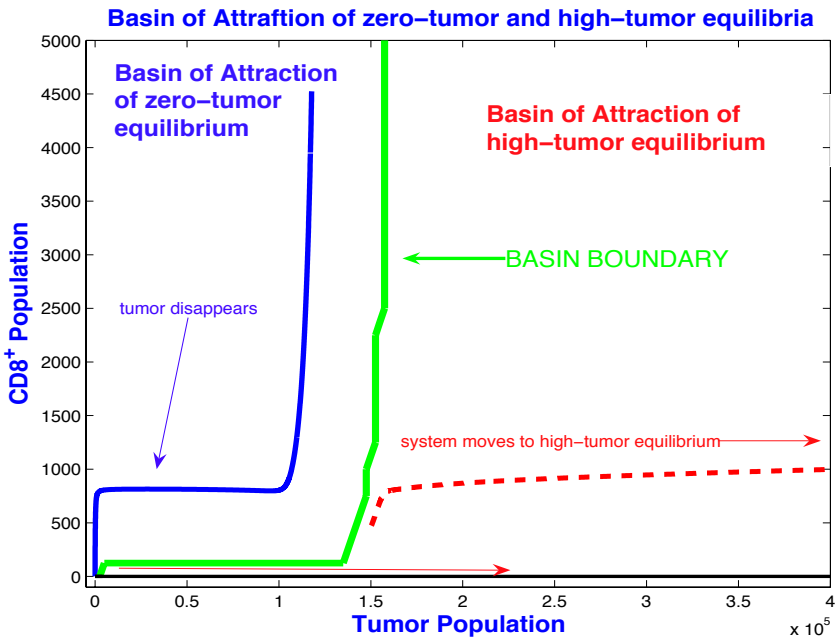


Fig. 5. Basins of attraction of the zero-tumor and high-tumor equilibria when the $CD8^+$ T-cell recruitment parameter, $j = 4.5$.

## 5 Numerical Experiments: Mouse Data with Immunotherapy, Chemotherapy and Combination Treatments

In this section, we test the behavior of our model using the data and results from a set of murine experiments presented in Diefenbach's work [26]. These data have also been employed in the simulations of de Pillis and Radunskaya's model [23]. We examine cases for which the immune system cannot fight a growing tumor on its own as well as cases for which neither chemotherapy nor immunotherapy alone can kill the tumor. We also present a case for which the administration of a combination of both chemotherapy and immunotherapy is necessary in order to cause a large tumor to die. For the following *in silico* experiments, we use the mouse parameters provided in Table 1.

### *5.1 Immune System Response to Tumor: Mouse Data*

In the first set of experiments for the mouse model, we present a situation in which the tumor escapes immuno-surveillance. The tumor reaches carrying capacity, and we assume the mouse dies under this extreme tumor burden. The initial conditions for this situation are chosen to be a tumor of size $10^6$ cells, a circulating lymphocyte population of $1.1 \times 10^7$, a natural killer cell population of $5 \times 10^4$, and a population of 100 $CD8^+$T cells. With the set of parameters in Table 1, the outcome of the simulation is sensitive to the initial conditions chosen. This set of initial conditions is meant to reflect a laboratory mouse experiment, in which an initial tumor challenge of $10^6$ cells is directly implanted into the mouse, and then the progression of the tumor is observed. Simulation results are presented in Figure 6, Top Left.

### *5.2 Chemotherapy or Immunotherapy: Mouse Data*

As seen, with parameters as currently set, a tumor challenge of size $10^6$ cells is too large for the innate immune system to control. The following set of experiments is useful for testing simulated treatment options.

The first treatment approach employs seven pulsed doses of chemotherapy, each dose represented by setting $v_M(t) = 1$ in equation (6) for one day, and given in a fourteen day cycle. The second treatment approach employs immunotherapy in the form of an injection of $8 \times 10^8$ highly activated $CD8^+$T cells from day 7 to day 8. This $CD8^+$ injection is meant to represent the TIL (tumor infiltrating lymphocyte) treatments used for certain patients (see, for example, [28]).

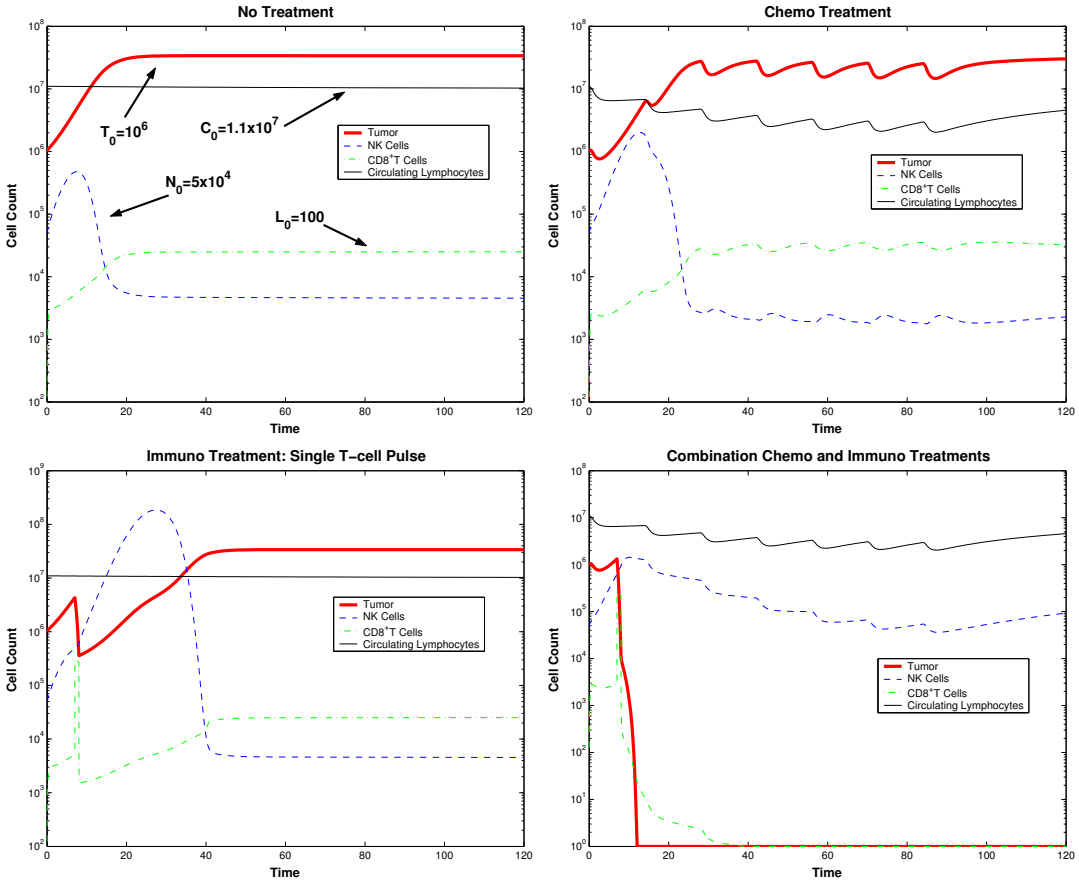


Fig. 6. Mouse data. **Top Left:** *No treatment.* Immune system without intervention where the tumor reaches carrying capacity and the mouse "dies". **Top Right:** *Chemotherapy.* The immune system response to high tumor with chemotherapy administered for one day in a fourteen day cycle. **Bottom Left:** *Immunotherapy.* Immune system response to high tumor with the administration of immunotherapy from days 7 to 8. **Bottom Right:** *Combination therapy.* Chemotherapy and immunotherapy as previously described given simultaneously effectively. control of the tumor. Parameters for all simulations are provided in Table 1.

For an initial tumor challenge of $10^6$ cells, the tumor survives despite either method of intervention. These experiments are pictured in Figure 6, Top Right and Bottom Left.

### *5.3 Combination Therapy: Mouse Data*

Some laboratory experiments have indicated the potential benefits of combining chemotherapy with immunotherapy (see, for example, [63]). In light of this, we

next present the results of an *in silico* experiment simulating combination therapy, displayed in the Bottom Right image in Figure 6. In this experiment, the chemotherapy and immunotherapy treatments outlined above are given simultaneously. Initial population sizes are set to the same values as in the previous experiments.

According to our model, combination therapy is far more effective in killing a tumor than either individual of treatment alone. We note that the drop in tumor population for this case is extremely steep. It is currently not clear whether the time scale for this tumor decline in response to combination therapy reflects realistic dynamics. However, the qualitative result highlights the synergistic effect of combination treatment, which does reflect the outcomes of certain studies (see, eg, [63,90]).

In some cases, if chemotherapy alone or immunotherapy alone are to be used effectively against tumor growth, it is thought that very high or more frequent doses must be employed. Higher medication levels can sometimes cause undesirable side-effects. Heavy chemotherapy will harm other tissues in the body, and too many TILs administered over a short period of time may be attacked and killed by suppressor immune cells before the TILs have a chance to significantly impact tumor cell growth. It seems reasonable that combination therapy that can employ lower doses of each therapy element has the potential to allow for faster tumor elimination with milder side-effects. The circulating lymphocyte level in the combination therapy experiment can be used to indicate that the immune health of the mouse has not suffered too greatly during treatment.

# 6 Numerical Experiments: Human Data with Immune, Chemo and Combination Treatments

In this section, we test the behavior of our model using parameters taken from experimental results of two patients from Rosenberg's study on metastatic melanoma [28]. In [28], both patients responded to treatment, so the *in silico* simulations here are experiments meant to explore various scenarios using human parameters.

First we examine the model with the set of parameters representing patient 9 in Table 2. We present a case for which a certain tumor burden can be controlled by a healthy immune system, but not by a slightly weakened immune system. We also present a case for which either chemotherapy alone or immunotherapy alone can kill a tumor, and a case for which a combination therapy is essential to the survival of the patient. We then compare the results using parameters from patient 9 of [28] to the simulated behavior of the model using patient 10 parameters of [28]. This patient comparison provides insight into patient-specific parameter sensitivity.

## *6.1 Immune System Response to Tumor: Human Data, Patient 9*

In the first set of human experiments, we examine an initial tumor burden of $10^6$ cells. This experiment represents a situation in which the immune system has not become activated against the tumor cell population until the population has reached $10^6$ cells, a size which in many cases is still considered to be below the threshold of clinical detectability in a human. For this tumor, immune system strength is very important in determining whether or not the body alone can kill a tumor. The first

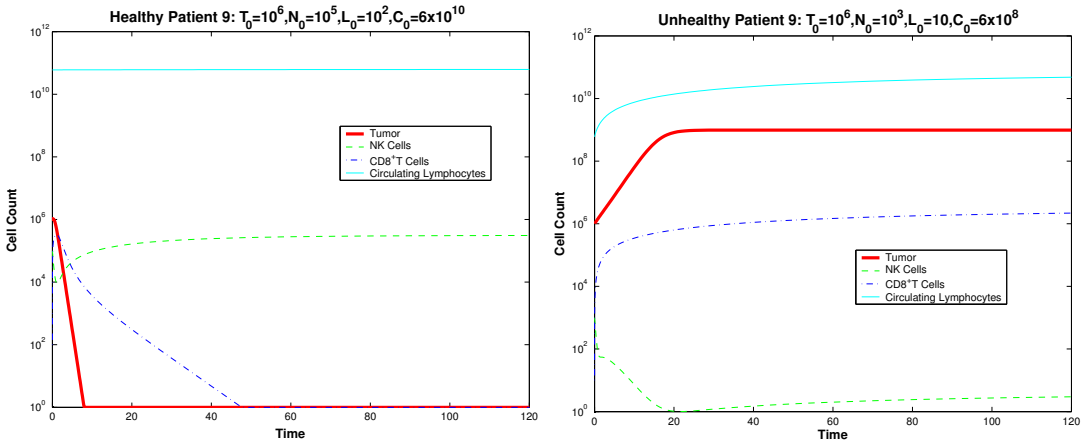


Fig. 7. Human data, Patient 9. **Left:** A healthy immune system effectively kills a small tumor. Initial Conditions: $1\times10^6$ Tumor cells, $1\times10^5$ NK cells, 100 CD8$^+$T cells, $6\times10^{10}$ circulating lymphocytes. **Right:** A depleted immune system fails to kill a small tumor when left untreated. Initial Conditions: $1\times10^6$ Tumor cells, $1\times10^3$ NK cells, 10 CD8$^+$T cells, $6\times10^8$ circulating lymphocytes. Parameters for these simulations are provided in Table 2.

experiment specifies what we will denote as an initially "healthy" immune system with $1\times10^5$ natural killer cells, $1\times10^2$ CD8$^+$T cells, and $6\times10^{10}$ circulating lymphocytes. As seen in Figure 7, Left, the innate immune response is sufficiently strong to control the tumor. However, when the immune system is weakened, a tumor of the same size grows to a dangerous level in the absence of treatment interventions. Simulated results for this weakened immune case, with initial conditions set to $1\times10^6$ tumor cells, $1\times10^3$ NK cells, 10 CD8$^+$T cells, and $6\times10^8$ circulating lymphocytes, are pictured in Figure 7, Right.

### *6.2 Chemotherapy: Human Data*

For cases in which the tumor would grow to a dangerous level if left untreated (such as in the depleted immune system example shown in Figure 7, Right), we model pulsed chemotherapy administration into the body, but only after the tumor is large enough to be considered potentially detectable. Examining the tumor's response to

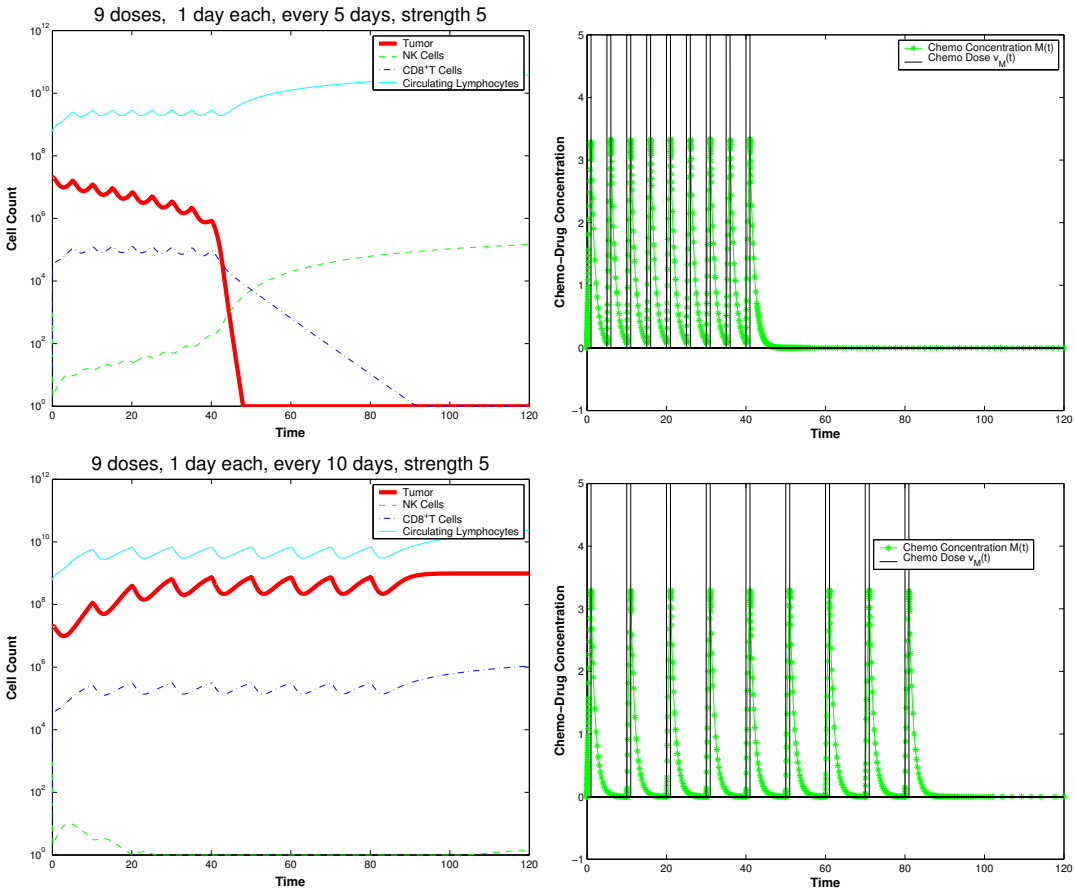


Fig. 8. Human data, Patient 9. **Top Left:** A case for which nine doses of chemotherapy over 45 days are sufficient to eliminate a tumor. Initial Conditions: $2 \times 10^7$ tumor cells, $1 \times 10^3$ NK cells, 10 CD8$^+$T cells, $6 \times 10^8$ circulating lymphocytes. **Top Right:** Drug administration pattern. Nine doses, strength $v_M(t) = 5$, one day per dose on a five day cycle. **Bottom Left:** A case where nine doses over 90 days is given and the tumor shows regrowth. Initial Conditions: $2 \times 10^7$ Tumor cells, $1 \times 10^3$ NK cells, 10 CD8$^+$T cells, $6 \times 10^8$ circulating lymphocytes. **Bottom Right:** Drug administration pattern: Nine doses, strength $v_M(t) = 5$, one day per dose on a ten day cycle. Parameters for these simulations are presented in Table 2.

pulsed chemotherapy given over different time courses, we determined that for a tumor burden of $2 \times 10^7$ cells, chemotherapy pulses administered once every five days are effective in killing the tumor, which dies by day 50 (see Figure 8, Top Left). The system is clearly sensitive to the chemotherapy dosing regimen. A treatment with the same total chemotherapy, but administered less frequently, once every 10 days (see Figure 8, Bottom Left) will allow the tumor to regrow.

### *6.3 Immunotherapy: Human Data*

In addition to pure chemotherapy treatments, we examine pure immunotherapy treatments. One of the major advantages of mathematical modeling is that while we can model therapies for which clinical trials have been performed (e.g., chemotherapy alone) thereby validating our model, we can also use our model to simulate theoretical treatment strategies, such as immunotherapy alone, a treatment approach not yet employed in most clinical trials. Our model parameters have been calibrated by comparing simulated outcomes to results from chemotherapy and combination therapy trials. Clinical trials for melanoma, against which we might at a future point directly compare simulations, are currently underway. (See, for example, [48] for a current list of ongoing trials.)

In this section we present *in silico* experiments with a TIL injection followed by short doses of IL-2. This mirrors the treatment that was given to patients 9 and 10 in Rosenberg's experiments [28], the difference being that the patients in the clinical trial were first administered immuno-depleting chemotherapy before the administration of TIL therapy.

In Figure 9, we investigate a $10^6$ cell tumor, a tumor level that the *in silico* innate immune system as specified cannot control on its own. However, as we have seen in our previous *in silico* experiments, a chemotherapy regimen can effectively handle this tumor challenge in patient 9. Figure 9, Left, shows the effect of immunotherapy alone against this tumor. The dosing of TILs and IL-2 administered here are the same as those shown in Figure 10. One advantage of this treatment approach is

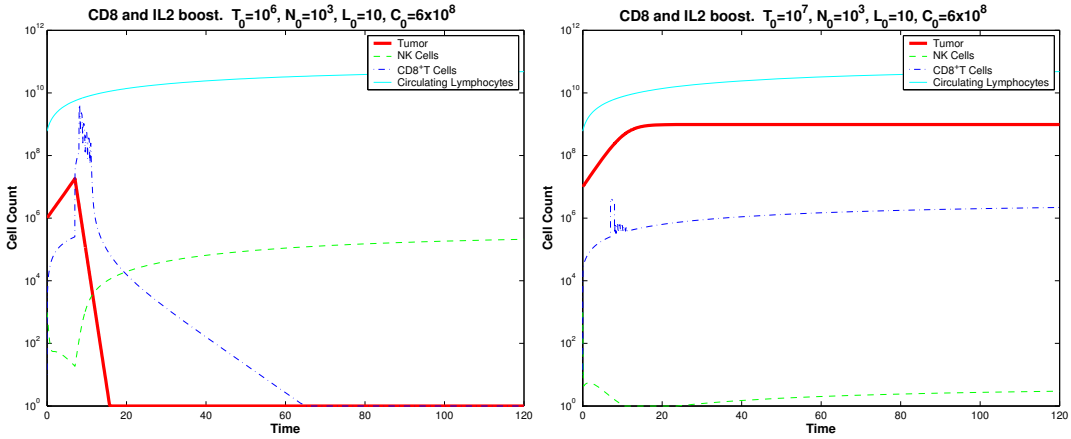


Fig. 9. Human data, Patient 9. **Left:** Immunotherapy is able to kill a tumor of size $10^6$ cells. $10^9$ TILs are administered from day 7 through 8. IL-2 is administered in 6 pulses at strength $5 \times 10^6$ from day 8 to day 11. **Right:** Immunotherapy is unable to kill a tumor of size $10^7$ cells. $10^9$ TILs are administered from day 7 through 8. IL-2 is administered in 6 pulses from day 8 to day 11. Parameters for these simulation are provided in Table 2.

that the immune system is directly strengthened, and not depleted as it is with chemotherapy.

We note that immunotherapy effectiveness may limited to smaller tumor sizes. Figure 9, Right, shows that immunotherapy alone is not effective in treating the tumor of size $10^7$. This size tumor could, instead, be cured by combination therapy, as is shown in Figure 10.

### *6.4 Combination Therapy*

While we have presented cases for which chemotherapy alone or immunotherapy alone can kill a tumor, there are situations in which these treatments in isolation are not sufficient to eliminate the tumor. We measure the patient's immunological health by the number of circulating lymphocytes in the body and do not allow the circulating lymphocytes to drop below a threshold where risk of infection may be

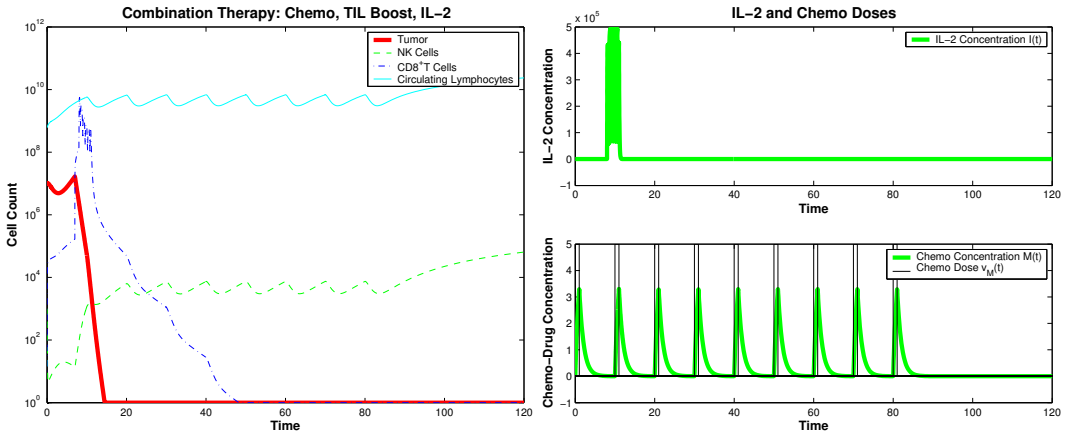


Fig. 10. Human data, Patient 9. Combining the separately unsuccessful therapies for a $10^7$ size tumor (see Figures 8, Bottom Left, and 9, Right) succeeds in eliminating the tumor. **Left:** A $10^7$ cell tumor is successfully eliminated by combining nine one-day chemotherapy doses of strength $v_M(t) = 5$ every 10 days, with a boost of TILs and IL-2. $10^9$ TILs are administered from day 7 through 8. IL-2 is administered in 6 pulses from day 8 to day 11 at concentration $v_I(t) = 5 \times 10^5$ per pulse. Initial conditions are as in previous simulations: $2 \times 10^7$ Tumor cells, $1 \times 10^3$NK cells, 10 CD8$^+$T cells, $6 \times 10^8$ circulating lymphocytes. Patient 9 parameters for these simulations are in Table 2. **Right:** Drug concentrations for IL-2 and chemotherapy.

too high. In our experiments, we chose that threshold to be on the order of $10^8$ cells. This amount reflects a fraction of approximate normal white blood cell levels in an adult human (see, e.g., [78]).

For the case in Figure 10, Left, combination treatment is now able to eliminate a tumor of $10^7$ cells. The combination treatment given is simply a superposition of the separate chemotherapy and immunotherapy regimens (unsuccessfully) applied in the previous experiments (see Figures 8, Bottom Left, and 9, Right). All initial conditions and parameter values remain the same as in these previous experiments. IL-2 and chemotherapy concentrations are provided in Figure 10, Right.

The simulation shown in Figure 10, Left, is consistent with the Rosenberg data [28] for patient 9, in the sense that patient 9 responded to treatment, and our simulation also reflects a positive response to combination therapy.

We performed multiple additional experiments, including those for which we examined the same combination therapy for tumors of sizes $10^8$ and larger. In these cases, the tumors were not controlled, except in certain cases for which additional doses of chemotherapy and IL-2 were given in varying combinations (figures not included).

### *6.5 Comparison with Patient 10*

In order to examine whether these treatment simulations vary from patient to patient, we change patient specific parameters extracted from Rosenberg's study, and run similar simulations with the parameters for patient 10 [28]. These parameters are given in Table 2.

First we repeat the experiment simulated in Figure 7 (no intervention) for a tumor of size $10^6$. In this case, the immune system conditions that killed the tumor in patient 9 are ineffective at managing the same size tumor in patient 10 (see Figure 11, Left). However, patient 10's immune system is able to handle a smaller tumor of size $10^5$ given the same initial immune cell count, as we show in Figure 11, Right. Clearly, the immune system's tumor handling capacity is patient specific. This is not surprising, since the combination therapy administered to thirteen patients in Rosenberg's study [28] gave rise to objective clinical responses in only six of the thirteen patients.

In addition to the differing results of the immune system alone, we examine the conditions under which combination therapy can control a $10^7$ size tumor in patient 10 with a compromised immune system (as specified by initial conditions). As opposed

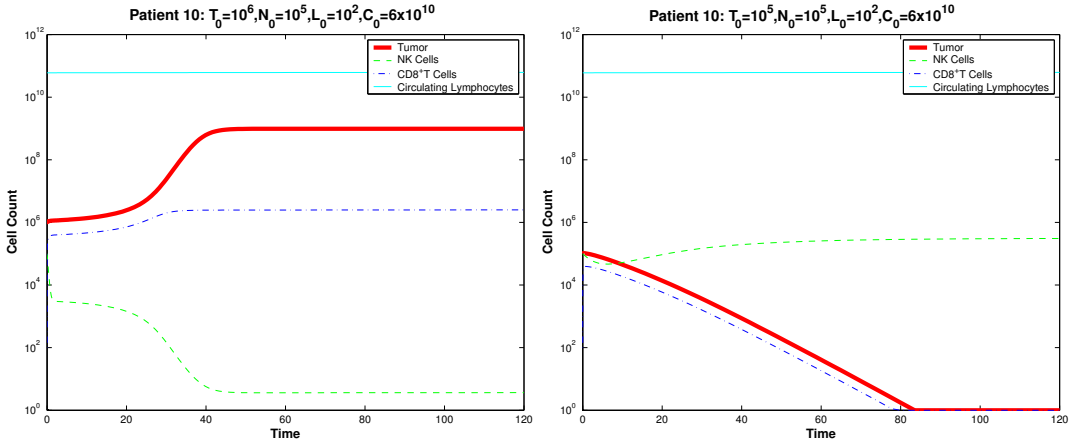


Fig. 11. Human data, Patient 10. **Left:** Patient 10 cannot kill a $10^6$ cell tumor with a healthy immune system of $10^5$ NK cells, 100 CD8$^+$T cells, and $6 \times 10^{10}$ circulating lymphocytes. **Right:** Patient 10 kills a $10^5$ cell tumor with a healthy immune system of $10^5$ NK cells, 100 CD8$^+$T cells, and $6 \times 10^{10}$ circulating lymphocytes. Patient parameters for these simulations are provided in Table 2.

to the positive outcome for patient 9 (see Figure 10), the parameter set for patient 10 leads to the growth of the tumor, as seen in in Figure 12, Top Left.

In this case, one treatment approach is to administer additional immunotherapy in the form of IL-2 doses. This expansion in treatment does lead to tumor death *in silico*, as shown in Figure 12, Top Right. We note in this case tumor behavior seems to reflect tumor dormancy followed by relapse. The tumor appears to have completely died out by day 22. However, around day 79, the tumor begins to re-emerge. Without the additional IL-2 treatment given at day 80, the tumor would regrow. We also ran the simulation for 2000 days, and the tumor did re-emerge, but at levels generally considered below detectability thresholds. The tumor subsequently died out again and did not reappear. See Figure 12, Bottom Left. This leads us to believe that the tumor population has been drawn into the stable zero tumor equilibrium at this point. Such a case in the clinic would likely be viewed as a successful case of complete remission.

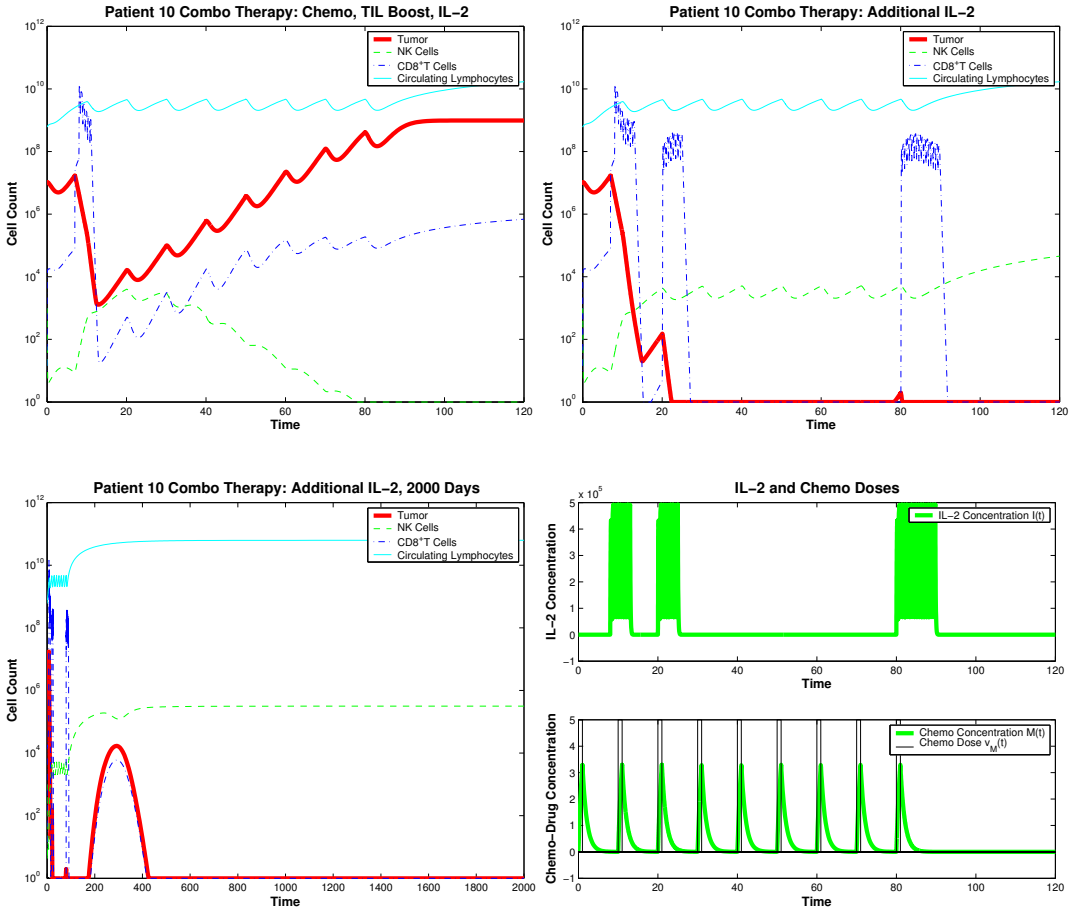


Fig. 12. Human data, Patient 10. **Top Left:** Combination therapy fails to eliminate the $10^7$ cell tumor in patient 10 with a compromised immune system of $10^3$ NK cells, 10 CD8$^+$T cells, and $6 \times 10^8$ circulating lymphocytes. $10^9$ TILs are administered from days 7 through 8. IL-2 is administered in 6 pulses from day 8 to day 11 at concentration $v_I(t) = 5 \times 10^6$ per pulse. **Top Right:** Combination therapy kills the $10^7$ cell tumor in patient 10. Treatment is identical to that in the Top Left panel, with the exception that pulses of IL-2 are administered from days 8 through 13, 20 through 25 and 80 through 90. **Bottom Left:** The same effective combination therapy as given in the Top Right panel and as shown in the Bottom Right panel, but viewed over 2000 days. **Bottom Right:** Concentrations for IL-2 and chemotherapy implemented in the simulations shown in the Top Right and Bottom Left panels. Patient 10 parameters are provided in Table 2.

## 7 Numerical Experiments: Human Data with Vaccine and Combination Treatments

In addition to T-cell boosts and IL-2 injections, we now simulate cancer vaccines. Cancer vaccines are a special case of immunotherapy for treating cancer. With a vaccine, the body is challenged with some modified form of the cancer, consequently

sensitizing the immune system to the presence of the cancer, allowing the immune system more effectively to find and lyse cancer cells.

### *7.1 Vaccine Therapy and a Change of Parameters*

In order to simulate vaccine therapy for human patients, we change the values of five parameters at the time of vaccination. These parameter changes are documented by the experimental data found in Diefenbach's results on mouse vaccine trials [26] and the experimental curves produced by these data are fitted to de Pillis's model [22]. According to these laboratory experiments in the context of our model, the parameters that would change to reflect the administration of a therapeutic vaccine are $c$, the fractional tumor cell kill by natural killer cells, $g$, the maximum NK-cell recruitment rate by tumor cells, $j$, the maximum $CD8^+$T cell recruitment rate, $s$, the steepness coefficient of the tumor-$CD8^+$T competition term, $d$, the saturation level of fractional tumor cell kill by $CD8^+$T cells, and $l$, the exponent of fractional tumor cell kill by $CD8^+$T cells. Of these six parameters, $l$ is the only one for which there is no clear relationship between its magnitude and the response of the system to vaccine, since this relationship is highly nonlinear and non-monotonic. We therefore leave $l$ unchanged, and focus on modifications to the remaining five parameters.

For this set of experiments, we use the patient 9 parameter set to simulate theoretical *in silico* vaccine therapy by altering parameters in the same direction as they change in Diefebach's murine model [26], [23]. We increase the values of $c$, $g$, $j$, and $d$ and decrease the value of $s$.

### *7.2 Vaccine and Chemotherapy Combination Experiments*

We first present a theoretical case in which a patient has a detectable tumor of size $2 \times 10^7$ and a "healthy" immune system of $3 \times 10^5$ NK cells, $10^2$ $CD8^+$T cells, and $10^{10}$ circulating lymphocytes. This is a case in which patient's immune system is not strong enough to handle a $10^7$ size tumor on its own (not pictured). As shown in Figure 13, Left, the body cannot handle this size tumor even when treated with aggressive pulsed chemotherapy for 50 days. Additionally, vaccine therapy, represented by changes to the original parameter set after 10 days, fails to control the tumor. This simulation is pictured in Figure 13, Middle. Only the combination of both treatments can kill a tumor of this magnitude, as shown in Figure 13, Right.

Such dramatic tumor regression is still uncommon among most patients, and sensitive to the choice of tumor and patient parameters, as well as to the timing of the treatments (see the next section). It has been noted, however, in the clinical studies of Wheeler [90], that over a period of 50 days, combination therapy provoked a drastic (¿50%) tumor regression in three of thirteen glioma patients. Wheeler points out that these tumor regression outcomes are rare in the literature. However, our model is able to describe these positive clinical responses to emerging combination therapies.

### *7.3 Vaccine Therapy Time Dependence*

There are cases for which vaccine therapy alone is able to control a growing tumor, but our simulations indicate that timing is an important factor in determining the

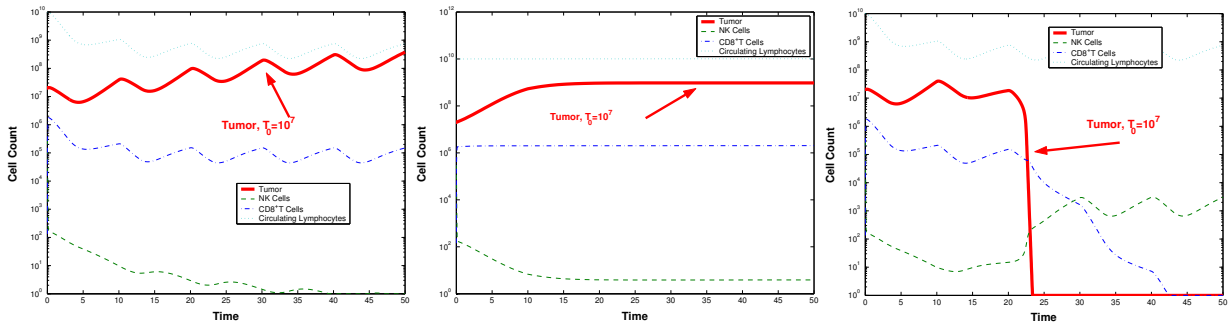


Fig. 13. Human data, Patient 10. **Left:** Chemotherapy alone cannot kill a $2 \times 10^7$ tumor with an immune system of $3 \times 10^5$ NK cells, 100 CD8$^+$T cells, and $10^{10}$ circulating lymphocytes. Chemotherapy at strength $v_M(t) = 2$ is administered for 3 consecutive days in a 10 day cycle. The parameters for this simulation are provided in Table 2. **Middle:** Vaccine therapy alone cannot control the tumor with the same initial conditions as given in Left figure. The parameters for this simulation are provided in Table 2, with parameters, modified after 10 days to reflect vaccine therapy, given by $c = 7.131 \times 10^{-9}, g = 0.5, j = 1, s = .0019, d = 15$. **Right:** Combination therapy effectively controls the tumor.

effectiveness of the vaccine treatment. Since we model vaccine therapy as a change in parameters, and not as a drug population, the amount of vaccine cannot be altered, but the timing of administration can be controlled. In the case for which an initial tumor is set to be half the size as that in the previous experiments ($10^7$ cells), and the immune system initial conditions are set to be the same, vaccine therapy effectively eliminates a tumor. However, this successful tumor elimination happens only if the vaccine is administered to the patient no more than 13 days after the tumor is hypothetically detected at $10^7$ tumor cells. If the vaccine is administered any later than that, it is ineffective. We show how the timing of vaccine therapy affects the final outcome in Figure 14.

## 8 Discussion and Conclusion

We have extended previous mathematical models that govern cancer growth with chemotherapy treatments to include immunotherapy and vaccine therapy. This

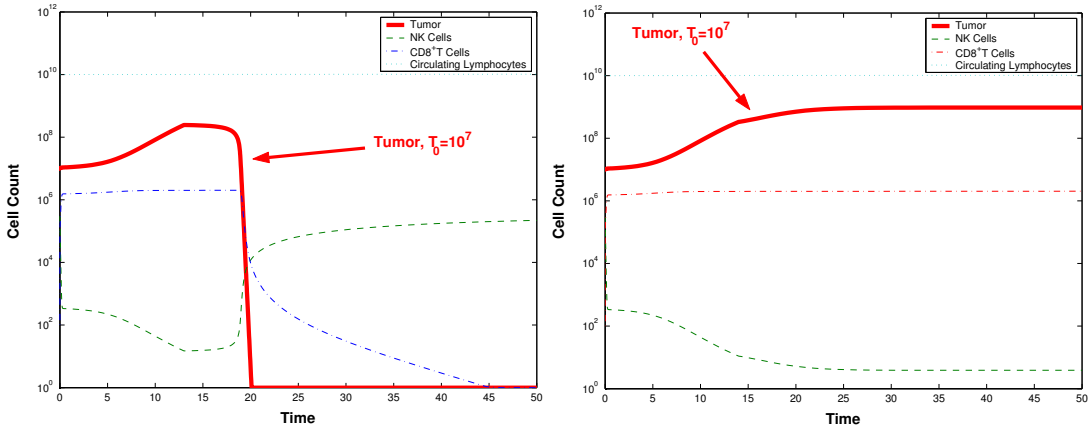


Fig. 14. Human data, Patient 10. **Left:** Vaccine administered after 13 days. The parameters for this simulation are provided in Table 2 with parameters modified on day 13 to reflect vaccine therapy given by $c = 7.131 \times 10^{-9}, g = 0.5, j = 1, s = .0019, d = 15$. **Right:** Vaccine administered on day 14, parameters modified as indicated.

structure can be used to test combination treatment approaches. The model is formulated as a system of ordinary differential equations that describe the global stimulatory effect of tumor cells on the immune response in conjunction with chemotherapies.

Through an analysis of the system of equations in the absence of chemotherapy or immunotherapy, we determined the equilibrium points of the system along with the criteria for stability. For a specific parameter set, we found two equilibria. One was a tumor-free equilibrium, which was shown to be unstable, and the other was a high-tumor equilibrium, shown to be stable. The instability of the tumor-free equilibrium implies that any successful treatment must be able to change the system parameters in order to force this desirable equilibrium point to become stable. The stability of the high-tumor equilibrium, on the other hand, implies that reducing the tumor burden through chemotherapy alone is not sufficient to drive the tumor level to zero. Once chemotherapy is stopped, a system with even an undetectable tumor remaining will eventually return to the high tumor state. However, system parameters may

be altered through treatments such as vaccination, thereby changing the stability nature of the zero tumor equilibrium, and allowing a combination treatment protocol to eliminate the patient's tumor. We note that in [36], a similar conclusion is reached through a different modeling approach: in this case, too, it is shown that unless system parameters are altered in some way, cytotoxic drugs alone are often not sufficient to control even a very small tumor.

A bifurcation analysis was performed for two of the system parameters. These analyses show that for certain parameter values, the long-term behavior of the system can be very sensitive to the initial conditions. One important implication of this result for tumor treatment is that if both the zero tumor and high tumor equilibrium points are stable then for cell populations that are close to the boundary separating the basins of attraction of these equilibria, very small changes in either the initial tumor size or the antigen-specific $CD8^+$T levels can have drastic consequences on the outcome of the disease. This would indicate that combination immuno-chemo therapies which push the system into the tumor-free basin of attraction should be employed to achieve a stable disease-free state.

Results of our model simulations have been validated by comparing the outcomes both to mouse [26] and to human [28] data. Simulations using parameter sets from two different patients show that treatment efficacy depends strongly on patient-specific characteristics. This observation may actually be used to our advantage: it is already possible to measure some of the significant patient specific parameters. In particular, through chromium release assays we can measure patient specific immune-tumor lysis rates, while tumor growth rates can also be measured in the

laboratory. We have seen that changes in these measurable parameters clearly affect system outcomes. As a result, although not all system parameters are yet measurable, those that are help to provide a good start in designing customized treatment protocols for each patient.

The development of combination immunotherapy-chemotherapy protocols for treating certain forms of cancer is an exciting new strategy in cancer treatment research. In some preliminary clinical studies, immunotherapy has been found to be most effective when administered in conjunction with chemotherapy [63], and this qualitative result has been borne out in our mathematical simulations. In this work, we have contributed to the emerging body of cancer modeling research by developing and analyzing a new mathematical model of cancer growth, immune response, and treatment that includes vaccine therapy, activated anticancer-cell transfer (TIL injections), and activation-protein injections (IL-2 injections) in combination with chemotherapy. The mathematical model presented in this paper should serve to enrich the study of cancer treatments and aid in guiding the development of new patient-specific combination treatment protocols.

## Acknowledgments

We would like to thank the following Harvey Mudd College students for their contributions to this work: Lindsay Crowl, Lorraine Thomas and Michael Vrable. This work was supported in part by the W.M. Keck Foundation and the National Science Foundation NSF-0414011.

## A: Nomenclature and Parameter Values

Here we list all of the parameters used in the model, their meaning and their estimated values. The first set of tables reflects the experiments run to simulate the mouse experiments from [26]. The second set of data applies to the human data from [28].

| Parameter | Units | Description | Estimated Value | Source |
|---|---|---|---|---|
| $a$ | $\text{day}^{-1}$ | Tumor growth rate. | $4.31 \times 10^{-1}$ | [26] |
| $b$ | $\text{cells}^{-1}$ | 1/b is tumor carrying capacity. | $2.17 \times 10^{-8}$ | [26] |
| $c$ | $\text{cell}^{-1}\cdot\text{day}^{-1}$ | Fractional (non)-ligand-transduced tumor cell kill by NK cells. | $7.13 \times 10^{-10}$ | [26] |
| $d$ | $\text{day}^{-1}$ | Saturation level of fractional tumor cell kill by $CD8^+T$ cells. Primed with ligand-transduced cells, challenged with ligand-transduced cells. | 8.17 | [26] |
| $l$ | none | Exponent of fractional tumor cell kill by $CD8^+T$ cells. Primed with ligand-transduced cells, challenged with ligand-transduced cells. | $6.57 \times 10^{-1}$ | [26] |
| $s$ | none | Steepness coefficient of the Tumor-($CD8^+T$ cell) lysis term $D$. Primed with ligand-transduced cells, challenged with ligand-transduced cells. (Smaller $s \Rightarrow$ steeper curve) | $6.18 \times 10^{-1}$ | [26] |
| $e$ | $\text{day}^{-1}$ | Fraction of circulating lymphocytes that become NK cells. | $1.29 \times 10^{-3}$ | [57] |
| $f$ | $\text{day}^{-1}$ | Death rate of NK cells. | $4.12 \times 10^{-2}$ | [57] |
| $g$ | $\text{day}^{-1}$ | Maximum NK cell recruitment rate by ligand-transduced tumor cells. | $4.98 \times 10^{-1}$ | [57], [26] |

| | | | | |
|---|---|---|---|---|
| $h$ | $\text{cell}^2$ | Steepness coefficient of the NK cell recruitment curve. | $2.02 \times 10^7$ | [57] |
| $p$ | $\text{cell}^{-1}\cdot\text{day}^{-1}$ | NK cell inactivation rate by Tumor cells. | $1.0 \times 10^{-7}$ | [26] |
| $m$ | $\text{day}^{-1}$ | Death rate of $CD8^+$T cells. | $2.0 \times 10^{-2}$ | [93] |
| $j$ | $\text{day}^{-1}$ | Maximum $CD8^+$T cell recruitment rate. Primed with ligand-transduced cells, challenged with ligand-transduced cells. | $9.96 \times 10^{-1}$ | [57], [26] |
| $k$ | $\text{cell}^2$ | Steepness coefficient of the $CD8^+$T cell recruitment curve. | $3.03 \times 10^5$ | [57], [26] |
| $q$ | $\text{cell}^{-1}\cdot\text{day}^{-1}$ | $CD8^+$T cell inactivation rate by Tumor cells. | $3.42 \times 10^{-10}$ | [57] |
| $r_1$ | $\text{cell}^{-1}\cdot\text{day}^{-1}$ | Rate at which $CD8^+$T cells are stimulated to be produced as a result of tumor cells killed by NK cells. | $1.1 \times 10^{-7}$ | [93], [59] |
| $r_2$ | $\text{cell}^{-1}\cdot\text{day}^{-1}$ | Rate at which $CD8^+$T cells are stimulated to be produced as a result of tumor cells interacting with circulating lymphocytes. | $3.0 \times 10^{-11}$ | No data found. |
| $u$ | $\text{cell}^{-2}\cdot\text{day}^{-1}$ | Regulatory function by NK-cells of $CD8^+$T-cells. | $1.80 \times 10^{-8}$ | No data found. |
| $K_T$ | $\text{day}^{-1}$ | Fractional tumor cell kill by chemotherapy. | $9.00 \times 10^{-1}$ | [76] |
| $K_N$, $K_L$, $K_C$ | $\text{day}^{-1}$ | Fractional immune cell kill by chemotherapy. | $6.00 \times 10^{-1}$ | [76] |
| $\alpha$ | $\text{cell}\cdot\text{day}^{-1}$ | Constant source of circulating lymphocytes. | $1.21 \times 10^5$ | [3,44] |
| $\beta$ | $\text{day}^{-1}$ | Natural death and differentiation of circulating lymphocytes. | $1.20 \times 10^{-2}$ | [3,44] |
| $\gamma$ | $\text{day}^{-1}$ | Rate of chemotherapy drug decay. | $9.00 \times 10^{-1}$ | [8] |

Table 1: Estimated mouse parameter values.

| Patient 9 | Patient 10 | Source |
|---|---|---|
| $a = 4.31 \times 10^{-1}$ | $a = 4.31 \times 10^{-1}$ | [26] |
| $b = 1.02 \times 10^{-9}$ | $b = 1.02 \times 10^{-9}$ | [26] |
| $c = 6.41 \times 10^{-11}$ | $c = 6.41 \times 10^{-11}$ | [28], [26] |
| $d = 2.34$ | $d = 1.88$ | [28] |
| $e = 2.08 \times 10^{-7}$ | $e = 2.08 \times 10^{-7}$ | [57] |
| $l = 2.09$ | $l = 1.81$ | [28] |
| $f = 4.12 \times 10^{-2}$ | $f = 4.12 \times 10^{-2}$ | [57] |
| $g = 1.25 \times 10^{-2}$ | $g = 1.25 \times 10^{-2}$ | [28], [26] |
| $h = 2.02 \times 10^{7}$ | $h = 2.02 \times 10^{7}$ | [57] |
| $j = 2.49 \times 10^{-2}$ | $j = 2.49 \times 10^{-2}$ | [28], [26] |
| $k = 3.66 \times 10^{7}$ | $k = 5.66 \times 10^{7}$ | [28], [26] |
| $m = 2.04 \times 10^{-1}$ | $m = 9.12$ | [93] |
| $q = 1.42 \times 10^{-6}$ | $q = 1.59 \times 10^{-6}$ | [57] |
| $p = 3.42 \times 10^{-6}$ | $p = 3.59 \times 10^{-6}$ | [26] |
| $s = 8.39 \times 10^{-2}$ | $s = 5.12 \times 10^{-1}$ | [28] |
| $r_1 = 1.10 \times 10^{-7}$ | $r_1 = 1.10 \times 10^{-7}$ | [93], [59] |
| $r_2 = 6.50 \times 10^{-11}$ | $r_2 = 6.50 \times 10^{-11}$ | No data found. |
| $u = 3.00 \times 10^{-10}$ | $u = 3.00 \times 10^{-10}$ | No data found. |
| $K_T = 9.00 \times 10^{-1}$ | $K_T = 9.00 \times 10^{-1}$ | [76] |
| $K_N = K_L = K_C = 6 \times 10^{-1}$ | $K_N = K_L = K_C = 6 \times 10^{-1}$ | [76] |

| | | |
|---|---|---|
| $\alpha = 7.50 \times 10^{8}$ | $\alpha = 5.00 \times 10^{8}$ | [3,44] |
| $\beta = 1.20 \times 10^{-2}$ | $\beta = 8.00 \times 10^{-3}$ | [3,44] |
| $\gamma = 9.00 \times 10^{-1}$ | $\gamma = 9.00 \times 10^{-1}$ | [8] |
| $p_I$: Maximum CD8$^+$T-cell recruitment rate by IL-2. Units: day$^{-1}$. | | |
| $p_I = 1.25 \times 10^{-1}$ | $p_I = 1.25 \times 10^{-1}$ | [54] |
| $g_I$: Steepness of CD8$^+$T-cell recruitment curve by IL-2. Units: cell$^2$. | | |
| $g_I = 2.00 \times 10^{7}$ | $g_I = 2.00 \times 10^{7}$ | [54] |
| $\mu_I$: Rate of IL-2 drug decay. Units: day$^{-1}$. | | |
| $\mu_I = 1.00 \times 10^{1}$ | $\mu_I = 1.00 \times 10^{1}$ | [54] |

Table 2: Estimated human parameter values.

## References


[1] J.A. Adam and N. Bellomo, editors. *A survey of models for tumor-immune system dynamics*, chapter Basic models of tumor-immune system interactions - Identification, analysis and predictions. Birkhauser, 1997.

[2] P.A. Antony and N.P. Restifo. CD4+CD25+ T regulatory cells, immunotherapy of cancer, and interleukin-2. *J Immunother.*, 28(2):120–128, Mar-Apr 2005.

[3] L. Bannock. Nutrition. Found at `http://www.doctorbannock.com/nutrition.html`.

[4] N. Bellomo, A. Bellouquid, and M. Delitala. Mathematical topics on the

modelling of multicellular systems in competition between tumor and immune cells. *Math Mod Meth Appl S.*, 14:1683–1733, 2004.

[5] N. Bellomo and L. Preziosi. Modelling and mathematical problems related to tumor evolution and its interaction with the immune system. *Math Comput Model.*, 32:413–452, 2000.

[6] J.N. Blattman and P.D. Greenberg. Cancer immunotherapy: A treatment for the masses. *Science*, 305:200–205, July 2004.

[7] N.F. Britton. *Essential Mathematical Biology.* Springer Verlag, 2003.

[8] P. Calabresi and P.S. Schein, editors. *Medical Oncology: Basic Principles and Clinical Management of Cancer.* McGraw-Hill, New York, second edition, 1993.

[9] R. Y. Chandawarkar and D. P. Guyton. Oncologic mathematics - evolution of a new specialty. *Arch Surg.*, 137:1428–1434, 2002.

[10] K. A. Chester, A. Mayer, J. Bhatia, L. Robson, D. I. R. Spencer, S. P. Cooke, A. A. Flynn, S. K. Sharma, G. Boxer, R. B. Pedley, and R. H. J. Begent. Recombinant anti-carcinoembryonic antigen antibodies for targeting cancer. *Cancer Chemother Pharmacol.*, 46:S8–S12, 2000.

[11] M.A. Cooper, T.A. Fehniger, and M.A. Caligiuri. The biology of human natural killer-cell subsets. *Trends Immunol.*, 22(11):633–640, 2001.

[12] J. Couzin. Select T cells, given space, shrink tumors. *Science*, 297:1973, September 2002.

[13] S. B. Cui. Analysis of a mathematical model for the growth of tumors under the action of external inhibitors. *J Math Biol.*, 44:395–426, 2002.

[14] B. Curti, A. Ochoa, W. Urba, G. Alvord, W. Kopp, G. Powers, C. Hawk, S. Creekmore, B. Gause, J. Janik, J. Holmlund, P. Kremers, R. Fenton, L. Miller, M. Sznol, J. Smith II, W. Sharfman, and D. Longo. Influence of interleukin-2 regimens on circulating populations of lymphocytes after adoptive transfer of anti-CD3-stimulated T cells: Results from a phase I trial in cancer patients. *J Immunother Emphasis Tumor Immunol.*, 19(4):296–308, July 1996.

[15] A. Dalgleish. The relevance of non-linear mathematics (chaos theory) to the treatment of cancer, the role of the immune response and the potential for vaccines. *QJM*, 92:347–359, 1999.

[16] A. G. Dalgleish and K. J. O'Byrne. Chronic immune activation and inflammation in the pathogenesis of AIDS and cancer. *Adv Cancer Res.*, 84:231–276, 2002.

[17] E. De Angelis and P.E. Jabin. Qualitative analysis of a mean field model of tumor-immune system competition. *Math Mod Meth Appl S.*, 13:187–206, 2003.

[18] E. De Angelis and L. Mesin. Modelling of the immune response: Conceptual frameworks and applications. *Math Mod Meth Appl S.*, 11:1609–1630, 2001.

[19] R.J. de Boer and P. Hogeweg. Interactions between macrophages and T-lymphocytes: tumor sneaking through intrinsic to helper T cell dynamics. *J Theor Biol.*, 120(3):331–51, June 1986.

[20] L. G. de Pillis and A. Radunskaya. The dynamics of an optimally controlled tumor model: A case study. *Math Comput Model.*, 37:1221–1244, 2003.

[21] L.G. de Pillis, A. Radunskaya, and C.L. Wiseman. A validated mathematical

model of cell-mediated immune responses to tumor invasion and vaccine therapy in mice and humans. Invited Poster, Society of Biological Therapy 17th Annual Meeting., 2003.

[22] L.G. de Pillis and A.E. Radunskaya. A mathematical tumor model with immune resistance and drug therapy: an optimal control approach. *J Theor Med.*, 3:79–100, 2001.

[23] L.G. de Pillis and A.E. Radunskaya. Immune response to tumor invasion. In K.J. Bathe, editor, *Computational Fluid and Solid Mechanics*, volume 2, pages 1661–1668, 2003. M.I.T.

[24] M. Delitala. Critical analysis and perspectives on kinetic (cellular) theory of immune competition. *Math Comput Model.*, 35:63–75, 2002.

[25] L. Derbel. Analysis of a new model for tumor-immune system competition including long time scale effects. *Math Mod Meth Appl S.*, 14:1657–1681, 2004.

[26] A. Diefenbach, E.R. Jensen, A.M. Jamieson, and D. Raulet. Rae1 and H60 ligands of the NKG2D receptor stimulate tumor immunity. *Nature*, 413:165–171, September 2001.

[27] J. Donnelly. Cancer vaccine targets leukemia. *Nat Med.*, 9(11):1354–1356, 2003.

[28] M.E. Dudley, J.R. Wunderlich, P.F. Robbins, J.C. Yang, P. Hwu, D.J. Schwartzentruber, S.L. Topalian, R. Sherry, N.P. Restifo, A.M. Hubicki, M.R. Robinson, M. Raffeld, P. Duray, C.A. Seipp, L. Rogers-Freezer, K.E. Morton, S.A. Mavroukakis, D.E. White, and S.A. Rosenberg. Cancer regression and autoimmunity in patients after clonal repopulation with antitumor

lymphocytes. *Science*, 298(5594):850–854, October 25 2002.

[29] J.D. Farrar, K.H. Katz, J. Windsor, G. Thrush, R.H. Scheuermann, J.W. Uhr, and N.E. Street. Cancer dormancy. VII. A regulatory role for CD8+ T cells and IFN-gamma in establishing and maintaining the tumor-dormant state. *J Immunol.*, 162(5):2842–9, March 1999.

[30] S. C. Ferreira, M. L. Martins, and M. J. Vilela. Reaction-diffusion model for the growth of avascular tumor. *Phys Rev E*, 65, 2002.

[31] S. W. Friedrich, S. C. Lin, B. R. Stoll, L. T. Baxter, L. L. Munn, and R. K. Jain. Antibody-directed effector cell therapy of tumors: Analysis and optimization using a physiologically based pharmacokinetic model. *Neoplasia*, 4:449–463, 2002.

[32] P. Garcia-Penarrubia, N. Lorenzo, J. Galvez, A. Campos, X. Ferez, and G. Rubio. Study of the physical meaning of the binding parameters involved in effector-target conjugation using monoclonal antibodies against adhesion molecules and cholera toxin. *Cell Immunol.*, 215:141–150, 2002.

[33] S. N. Gardner. A mechanistic, predictive model of dose-response curves for cell cycle phase-specific and nonspecific drugs. *Cancer Res.*, 60:1417–1425, 2000.

[34] R.A. Gatenby and E. T. Gawlinski. The glycolytic phenotype in carcinogenesis and tumor invasion: Insights through mathematical models. *Cancer Res.*, 63:3847–3854, 2003.

[35] R.A. Gatenby and P. K. Maini. Modelling a new angle on understanding cancer. *Nature*, 410:462, December 2002.

[36] R.A. Gatenby and T.L. Vincent. Application of quantitative models from population biology and evolutionary game theory to tumor therapeutic strategies. *Mol Cancer Ther.*, 2(9):919–927, September 2003.

[37] R.N. Germain. An innately interesting decade of research in immunology. *Nat Med.*, 10(12):1307–1320, December 2004.

[38] A. Gett, F. Sallusto, A. Lanzavecchia, and J. Geginat. T cell fitness determined by signal strength. *Nat Immunol.*, 4(4):355–360, April 2003.

[39] S.M. Gilbertson, P.D. Shah, and D.A. Rowley. NK cells suppress the generation of Lyt-2+ cytolytic T cells by suppressing or eliminating dendritic cells. *J Immunology*, 136(10):3567–3571, May 1986.

[40] R. Glas, L. Franksson, C. Une, M. Eloranta, C. Ohlen, A. Orn, and K. Karre. Recruitment and activation of natural killer (NK) cells in vivo determined by the target cell phenotype: An adaptive component of NK cell-mediated responses. *J. Exp. Med.*, 191(1):129–138, 2000.

[41] T.A. Hadj. Alemtuzumab for B-cell chronic lymphocytic leukemia. *Issues Emerg Health Technol.*, 66:1–4, Mar 2005.

[42] I. Hara, H. Hotta, N. Sato, H. Eto, S. Arakawa, and S. Kamidono. Rejection of mouse renal cell carcinoma elicted by local secretion of interleukin-2. *Jpn J Cancer Res.*, 87(7):724–729, July 1996.

[43] K. Hardy and J. Stark. Mathematical models of the balance between apoptosis and proliferation. *Apoptosis*, 7:373–381, 2002.

[44] B. Hauser. Blood tests. Technical report, International Waldenstrom's

Macroglobulinemia Foundation, January 2001. Available at http://www.iwmf.com/Blood_Tests.pdf Accessed May 2005.

[45] J.F. Holland and F. Emil III, editors. *Cancer Medicine*, chapter II-3, XII, XV. Lea and Febiger, 1973.

[46] A.Y.C. Huang, P. Golumbek, M. Ahmadzadeh, E. Jaffee, D. Pardoll, and H. Levitsky. Role of bone marrow-derived cells in presenting MHC class I-restricted tumor antigens. *Science*, 264(5161):961–965, May 1994.

[47] Cancer Research Institute. Cancer and the immune system: The vital connection. Web page publication of the Cancer Research Institute, 2000. Available at http://www.cancerresearch.org/immunology/immuneindex.html Accessed May 2005.

[48] National Cancer Institute. National cancer institute clinical trials web site. Available at http://www.nci.nih.gov/clinicaltrials Accessed May 2005.

[49] National Cancer Institute. Understanding chemotherapy. Available at http://www.nci.nih.gov/cancertopics/chemotherapy-and-you/page2. Accessed May 2005.

[50] H. Jiang and L. Chess. An integrated view of supporessor T cell subsets in immunoregulation. *J Clin Invest.*, 114(9):1198–1208, November 2004.

[51] Y. Kawarada, R. Ganss, N. Garbi, B. Sacher, T. ad Arnold, and G. Hammerling. NK- and CD8+T cell-mediate eradication of established tumors by peritumoral injection of CpG-containing oligodeoxynucleotides. *J Immunol.*, 167(1):5247–5253, 2001.

[52] D. Keil, R. W. Luebke, and S. B. Pruett. Quantifying the relationship between multiple immunological parameters and host resistance: Probing the limits of reductionism. *J Immunol.*, 167:4543–4552, 2001.

[53] W.C. Kieper, M. Prlic, C.S. Schmidt, M.F. Mescher, and S.C. Jameson. Il-12 enhances CD8 T cell homeostatic expansion. *J Immunol.*, 166:5515–5521, 2001.

[54] D. Kirschner and J.C. Panetta. Modeling immunotherapy of the tumor-immune interaction. *J Math Biol.*, 37(3):235–52, September 1998.

[55] M. Kolev. Mathematical modelling of the competition between tumors and immune system considering the role of the antibodies. *Math Comput Model.*, 37:1143–1152, 2003.

[56] V. Kuznetsov and I. Makalkin. Bifurcation-analysis of mathematical-model of interactions between cytotoxic lymphocytes and tumor-cells – effect of immunological amplification of tumor-growth and its connection with other phenomena of oncoimmunology. *Biofizika*, 37(6):1063–70, November-December 1992.

[57] V. Kuznetsov, I. Makalkin, M. Taylor, and A. Perelson. Nonlinear dynamics of immunogenic tumors: Parameter estimation and global bifurcation analysis. *Bulletin of Mathematical Biology*, 56(2):295–321, 1994.

[58] V. A. Kuznetsov and G. D. Knott. Modeling tumor regrowth and immunotherapy. *Math Comput Model.*, 33:1275–1287, 2001.

[59] A. Lanzavecchia and F. Sallusto. Dynamics of T-lymphocyte responses: Intermediates, effectors, and memory cells. *Science*, 290:92–97, 6 Oct 2000.

[60] J. Li, K. Guo, V.W. Koh, J.P. Tang, B.Q. Gan, H. Shi, H.X. Li, and Q. Zeng. Generation of PRL-3- and PRL-1-specific monoclonal antibodies as potential diagnostic markers for cancer metastases. *Clin Cancer Res.*, 11(6):2195–2204, Mar 2005.

[61] U. Lucia and G. Maino. Thermodynamical analysis of the dynamics of tumor interaction with the host immune system. *Physica A*, 313:569–577, 2002. doi:10.1016/S0378-4371(02)00980-9.

[62] A. Lumsden, J. Codde, P. Van Der Meide, and B. Gray. Immunohistochemical characterisation of immunological changes at the tumour site after chemo-immunotherapy with doxorubicin, interleukin-2 and interferon-$\gamma$. *Anticancer Res.*, 167(7):1145–1154, 1996.

[63] J. Machiels, R.T. Reilly, L.A. Emens, A.M. Ercolini, R.Y. Lei, D. Weintraub, F.I. Okoye, and E.M. Jaffee. Cyclophosphamide, doxorubicin, and paclitaxel enhance the antitumor immune response of granulocyte/macrophage-colony stimulating factor-secreting whole-cell vaccines in HER-2/*neu* tolerized mice. *Cancer Res.*, 61(9):3689–3697, May 2001.

[64] F. M. Marincola, E. Wang, M. Herlyn, B. Seliger, and S. Ferrone. Tumors as elusive targets of T-cell-based active immunotherapy. *Trends Immunol.*, 24:335–342, 2003.

[65] B. Melichar, J. Dvorak, P. Jandik, M. Touskova, D. Solichova, J. Megancova, and Voboril Z. Intraarterial chemotherapy of malignant melanoma metastatic to the liver. *Hepatogastroenterology*, 48(42):1711–1715, 2001.

[66] S. Morecki, T. Pugatsch, S. Levi, Y. Moshel, and S. Slavin. Tumor-cell vaccination induces tumor dormancy in a murine model of B-cell leukemia/lymphoma (BCL1). *Int J Cancer*, 65(2):204–8, 1996.

[67] M. Muller, F. Gounari, S. Prifti, H.J. Hacker, V. Schirrmacher, and K. Khazaie. EblacZ tumor dormancy in bone marrow and lymph nodes: active control of proliferating tumor cells by CD8+ immune T cells. *Cancer Res.*, 58(23):5439–46, December 1998.

[68] M.M. Mustafa, G.R. Buchanan, N.J. Winick, G.H. McCracken, I. Tkaczewski, M. Lipscomb, Q. Ansari, and M.S. Agopian. Immune recovery in children with malignancy after cessation of chemotherapy. *J Pediatr Hematol Oncol.*, 20(5):451–457, 1998.

[69] F. Nani and H. I. Freedman. A mathematical model of cancer treatment by immunotherapy. *Math Biosci.*, 163:159–199, 2000.

[70] K. J. O'Byrne, A. G. Dalgleish, M. J. Browning, W. P. Steward, and A. L. Harris. The relationship between angiogenesis and the immune response in carcinogenesis and the progression of malignant disease. *Eur J Cancer.*, 36:151–169, 2000.

[71] T. Osada, H. Nagawa, and Y. Shibata. Tumor-infiltrating effector cells of $\alpha$-galactosylceramide-induced antitumor immunity in metastatic liver tumor. *J Immune Based Ther Vaccines.*, 2(7):1–9, July 2004.

[72] M. R. Owen and J. A. Sherratt. Mathematical modelling of macrophage dynamics in tumours. *Math Mod Meth Appl S.*, 9:513–539, 1999.

[73] D.M. Pardoll. Cancer vaccines. *Nat Med.*, 4(5):525–531, May 1998. Vaccine Supplement.

[74] R. Pazdur, W. Hoskins, L. Wagman, and L. Coia, editors. *Cancer Management: A Mulitdisciplinary Approach*, chapter Principles of Chemotherapy. Oncology Publishing Group of CMP Healthcare Media, eighth edition, 2004. Available at `http://www.cancernetwork.com/handbook/contents.htm` Accessed May 2005.

[75] A.S. Perelson and G. Weisbuch. Immunology for physicists. *Rev Mod Phys.*, 69(4):1219–1267, October 1997.

[76] M.C. Perry, editor. *The Chemotherapy Source Book*. Lippincott Williams & Wilkins, third edition, 2001.

[77] Z. Qu, G.L. Griffiths, W.A. Wegener, C.H. Chang, Govindan S.V., I.D. Horak, H.J. Hansen, and D.M. Goldenberg. Development of humanized antibodies as cancer therapeutics. *Methods*, 36(1):84–95, May 2005. doi:10.1016/j.ymeth.2005.01.008.

[78] I.M. Roitt, J. Brostoff, and D.K. Male. *Immunology*. Mosby, St. Louis, 1993.

[79] E. Rosenbaum and I. Rosenbaum. *Everyone's Guide to Cancer Supportive Care: A Comprehensive Handbook for Patients and Their Families*. Andrews McMeel Publishing, 2005.

[80] S. Rosenberg and M. Lotze. Cancer immunotherapy using interleukin-2 and interleukin-2-activated lymphoytes. *Annu Rev Immunol.*, 4:681–709, 1986.

[81] S.A. Rosenberg, J.C. Yang, and N.P. Restifo. Cancer immunotherapy: Moving beyond current vaccines. *Nat Med.*, 10(9):909–915, September 2004.

[82] R.A. Sharma, A. G. Dalgleish, W. P. Steward, and K. J. O'Byrne. Angiogenesis and the immune response as targets for the prevention and treatment of colorectal cancer (review). *Oncol Rep.*, 10:1625–1631, 2003.

[83] O. Sotolongo-Costa, L.M. Molina, D.R. Perez, J.C. Antoranz, and M.C. Reyes. Behavior of tumors under nonstationary therapy. *Physica D*, 178:242–253, 2003. doi:10.1016/S0167-2789(03)00005-8.

[84] R. F. Stengel, R. Ghigliazza, N. Kulkarni, and O. Laplace. Optimal control of innate immune response. *Optim Contr Appl Met.*, 23:91–104, 2002.

[85] T.H. Stewart. Immune mechanisms and tumor dormancy. *Medicina - Buenos Aire*, 56(1):74–82, 1996.

[86] T. Takayanagi and A. Ohuchi. A mathematical analysis of the interactions between immunogenic tumor cells and cytotoxic t lymphocytes. *Microbiol Immunol.*, 45:709–715, 2001.

[87] R. Wallace, D. Wallace, and R. G. Wallace. Toward cultural oncology: The evolutionary information dynamics of cancer. *Open Syst Inf Dyn*, 10:159–181, 2003.

[88] S. D. Webb, J. A. Sherratt, and R. G. Fish. Cells behaving badly: a theoretical model for the Fas/FasL system in tumour immunology. *Math Biosci.*, 179:113–129, 2002.

[89] L. M. Wein, J. T. Wu, and D. H. Kirn. Validation and analysis of a

mathematical model of a replication-competent oncolytic virus for cancer treatment: Implications for virus design and delivery. *Cancer Res.*, 63:1317–1324, 2003.

[90] C.J. Wheeler, D. Asha, L. Gentao, J.S. Yu, and K.L. Black. Clinical responsiveness of glioblastoma multiforme to chemotherapy after vaccination. *Clin Cancer Res.*, 10:5316–5326, August 2004.

[91] D. Wodarz. Viruses as antitumor weapons: Defining conditions for tumor remission. *Cancer Res.*, 61:3501–3507, 2001.

[92] D. Wodarz and V. A. A. Jansen. A dynamical perspective of ctl cross-priming and regulation: implications for cancer immunology. *Immunol Lett.*, 86:213–227, 2003.

[93] A. Yates and R. Callard. Cell death and the maintenance of immunological memory. *Discret Contin Dyn S.*, 1(1):43–59, 2002.